Fungal Genetics and Biology 96 (2016) 33–46

Contents lists available at ScienceDirect

Fungal Genetics and Biology

journal homepage: www.elsevier.com/locate/yfgbi

Regular Articles

# The botrydial biosynthetic gene cluster of *Botrytis cinerea* displays a bipartite genomic structure and is positively regulated by the putative $Zn(II)_2Cys_6$ transcription factor BcBot6

Antoine Porquier [a,b], Guillaume Morgant [b], Javier Moraga [c], Bérengère Dalmais [b], Isabelle Luyten [d], Adeline Simon [b], Jean-Marc Pradier [b], Joëlle Amselem [d], Isidro González Collado [c,1], Muriel Viaud [b,*,1]

[a] Université Paris-Sud, 91405 Orsay, France
[b] UMR BIOGER, INRA, AgroParisTech, Université Paris-Saclay, 78850 Thiverval-Grignon, France
[c] Departamento de Química Orgánica, Facultad de Ciencias, Universidad de Cádiz, 11510 Puerto Real, Cádiz, Spain
[d] URGI, INRA, Université Paris-Saclay, 78026 Versailles, France

ARTICLE INFO

*Article history:*
Received 28 July 2016
Revised 30 September 2016
Accepted 5 October 2016
Available online 6 October 2016

*Keywords:*
*Botrytis cinerea*
Secondary metabolism
Toxin
Botrydial
Transcription factor
$Zn(II)_2Cys_6$

ABSTRACT

Botrydial (BOT) is a non-host specific phytotoxin produced by the polyphagous phytopathogenic fungus *Botrytis cinerea*. The genomic region of the BOT biosynthetic gene cluster was investigated and revealed two additional genes named *Bcbot6* and *Bcbot7*. Analysis revealed that the G + C/A + T-equilibrated regions that contain the *Bcbot* genes alternate with A + T-rich regions made of relics of transposable elements that have undergone repeat-induced point mutations (RIP). Furthermore, BcBot6, a $Zn(II)_2Cys_6$ putative transcription factor was identified as a nuclear protein and the major positive regulator of BOT biosynthesis. In addition, the phenotype of the *ΔBcbot6* mutant indicated that BcBot6 and therefore BOT are dispensable for the development, pathogenicity and response to abiotic stresses in the *B. cinerea* strain B05.10. Finally, our data revealed that *B. pseudocinerea*, that is also polyphagous and lives in sympatry with *B. cinerea*, lacks the ability to produce BOT. Identification of BcBot6 as the major regulator of BOT synthesis is the first step towards a comprehensive understanding of the complete regulation network of BOT synthesis and of its ecological role in the *B. cinerea* life cycle.



## 1. Introduction

Filamentous fungi are well-known producers of so-called secondary metabolites (SMs) or natural products, many of which confer either beneficial or detrimental properties. For example, the polyketide lovastatin is widely used as an anti-cholesterol drug (Manzoni and Rollini, 2002) whereas aflatoxin is carcinogenic and is a threat for both humans and animals (Hoffmeister and Keller, 2007). These molecules, generally of low molecular weight, can be considered as conditional for fungal growth and their production is often linked to developmental programs (Calvo et al., 2002). In most cases, their role is unknown but some studies demonstrate their importance for protecting fungi *e.g.* against predation (Rohlfs and Churchill, 2011) or to survive in hostile environment (Eisenman and Casadevall, 2012). Unique features of the genes involved in SM biosynthesis is their genomic co-localization (Smith et al., 1990; Keller and Hohn, 1997; Hoffmeister and Keller, 2007) as well as their co-regulation (Yin and Keller, 2011).

To be able to finely respond to different stimuli, fungi have evolved sophisticated gene regulation mechanisms. In particular, the ability of fungi to produce SMs during orchestrated time and in different environments implies complex hierarchical regulatory mechanisms. Around 60% of known fungal secondary metabolism gene clusters possess a pathway specific transcription factor (TF; Brakhage, 2012). In general, those proteins belong to the $Zn(II)_2Cys_6$ TF family and specifically regulate the genes of their corresponding cluster (Knox and Keller, 2015).

In addition to a specific type of regulators, broad domain TFs are involved in the regulation of fungal genes involved in SMs produced in response to environmental stimuli (*e.g.* pH, carbon and

*Abbreviations:* SM, secondary metabolite; BOT, botrydial; BOA, botcinic acid; PKS, polyketide synthase; TF, transcription factor; TE, transposable element; RIP, repeat-induced point mutation; GFP, green fluorescent protein; HPLC, High-pressure liquid chromatography, NMR, Nuclear Magnetic Resonance.

* Corresponding author.
*E-mail address:* viaud@versailles.inra.fr (M. Viaud).
[1] Co-senior authors.

http://dx.doi.org/10.1016/j.fgb.2016.10.003
1087-1845/

nitrogen source or redox status) (Brakhage, 2012). One example is the GATA TF AreA that regulates different clusters in diverse fungal species according to the available nitrogen source (Tudzynski et al., 1999; Kim and Woloshuk, 2008; Tudzynski, 2014).

Even though the action of TFs is necessary to regulate fungal SM genes, it is not always sufficient. Indeed, chromatin is a dynamic structure that can switch from the transcriptionally permissive euchromatin (opened state) to the repressive heterochromatin (condensed state) and *vice versa* (Palmer and Keller, 2010). This process is mediated by post-translational modifications of histone residues such as the trimethylation of the lysine 9 residue of histone 3 (H3K9me3) deposited by DIM-5 in *Neurospora crassa* (Tamaru and Selker, 2001). The presence of H3K9me3 mark is often associated with A + T-rich sequences that result through a process known as RIP for Repeat-Induced Point mutations (Hane et al., 2015). This pre-meiotic defense system aims to protect the genome from invasive elements such as transposable elements (TEs) or viruses by mutating C to T bases within duplicated sequences.

The putative methyltransferase LaeA is another important global regulator of SM in fungi is the putative methyltransferase LaeA. This nuclear protein interacts with VeA and VelB to form the fungal specific Velvet complex that mediates development and SM genes expression in response to light (Bayram et al., 2008). The mode of action of LaeA is currently unknown but a study in *Aspergillus nidulans* by Reyes-Dominguez et al. (2010) suggests that it might counteract the establishment of the repressive H3K9me3 mark and thereby have an impact on chromatin structure.

*Botrytis cinerea* is an Ascomycetous necrotrophic fungus that induces gray mold disease on more than 1400 plant species (Elad et al., 2016). This fungus is considered as one of the most important fungal plant pathogens and causes important economic losses on grapevine and many other fruits and flowers (Dean et al., 2012). Numerous SMs have been isolated from *B. cinerea* fermentation cultures (Collado et al., 2007; Collado and Viaud, 2016) including two non-host specific phytotoxins: the sesquiterpene botrydial (BOT) and its derivatives (botryanes) as well as the polyketide botcinic acid (BOA) and the structurally related botcinins. The genes involved in the production of both BOT and BOA are organized in clusters within the *B. cinerea* genome. The BOT gene cluster contains five genes encoding biosynthesis enzymes. *Bcbot2* encodes a sesquiterpene cyclase which is the first fungal key enzyme demonstrated to be able to convert farnesyl pyrophosphate into presilphiperfolan-8-beta-ol (Pinedo et al., 2008). *Bcbot1*, *Bcbot3* and *Bcbot4* encode cytochrome P450 proteins. Finally, *Bcbot5* encodes a putative acetyl transferase probably also involved in the biosynthesis of the toxin (Siewers et al., 2005; Collado and Viaud, 2016). The BOA cluster is composed of sixteen predicted genes with two encoding the polyketide synthase (PKS) key enzymes (namely *Bcboa6* and *Bcboa9*), ten encoding enzymes putatively involved in the further steps of the biosynthesis and two encoding putative regulators: a putative NmrA-like regulator (*Bcboa1*) and a putative specific regulator encoding a $Zn(II)_2Cys_6$ TF (*Bcboa13*) (Dalmais et al., 2011).

Both BOT and BOA are phytotoxic. BOT is produced during infection *in planta* (Deighton et al., 2001) and has been shown to induce chlorosis symptoms typical of the gray mold when applied exogenously (Rebordinos et al., 1996; Colmenares et al., 2002). Dihydrobotrydial and other derivatives also display phytotoxic activity but to a lesser extent than BOT (Durán-Patrón et al., 1999; Colmenares et al., 2002; Collado and Viaud, 2016). In the same manner, exogenous application of BOA and derivatives leads to chlorosis and necrosis on different plant hosts underlying their phytotoxic activity (Cutler et al., 1993, 1996). Inactivation of both *Bcbot2* and *Bcboa6* and the subsequent absence of BOT and BOA production showed that these toxins are involved in the colonization of plant tissues (Dalmais et al., 2011). Nevertheless, their mode of action remains enigmatic and only scarce information is available regarding their regulation.

To date it has been demonstrated that both BOA and BOT gene clusters are under the control of two signal transduction pathways. The first one cascade involves BCG1 α subunit of a heterotrimeric G protein, phospholipase C (BcPlc1), calcineurin phosphatase and the downstream $C_2H_2$ TF BcCrz1 (Viaud et al., 2003; Pinedo et al., 2008; Schumacher, 2008a, 2008b; Dalmais et al., 2011). The second is the stress-induced MAP kinase cascade (Heller et al., 2012) with the downstream bZIP TF BcAtf1 (Temme et al., 2012) and the BcReg1 transcriptional regulator (Michielse et al., 2011). In addition, it was demonstrated that *B. cinerea* secondary metabolism is greatly influenced by light-dependent development (Viaud et al., 2016). In *B. cinerea*, the perception of light triggers the production of macroconidia and represses the formation of sclerotia. This developmental program involves the members of the Velvet complex BcVel1, BcVel2 and BcLae1 (the orthologs of VeA, VelB and LaeA, respectively) (Schumacher et al., 2012, 2015; Yang et al., 2013). The deletion of the Velvet partners leads to abnormal constant production of conidia even in sclerotia-inducing conditions *i.e.* darkness, increase in conidial melanin (Schumacher, 2016), loss of oxalic acid formation and reduced virulence. In addition, sixteen SM gene clusters are affected by either deletion of *Bcvel1* or *Bclae1* or by both. In particular, the BOT and BOA gene clusters were shown to be positively regulated by BcLae1.

The gene deletion of all the regulators presented above results in pleiotropic phenotypes and does not point to specific regulation of the biosynthesis of the BOT and BOA phytotoxins. As introduced above, the gene *Bcboa13* located in the BOA gene cluster is predicted to encode a $Zn(II)_2Cys_6$ TF and is likely a pathway specific regulator (Dalmais et al., 2011). In contrast, no gene encoding a putative regulator has been identified to date in the BOT gene cluster. To find a BOT specific regulator, Simon et al. (2013) constructed a Yeast One Hybrid library containing nearly all *B. cinerea* TFs (396 out of the 406 predicted TFs). The screening of the library using the bidirectional promoter of *Bcbot1-2* as bait led to the identification of the $C_2H_2$ TF BcYoh1. A global transcriptomic analysis of the *ΔBcyoh1* mutant revealed this TF to be a global transcriptional regulator not only acting on the BOT and other SM gene clusters but also on carbohydrate metabolism, transport, virulence and detoxification mechanisms.

Until this report, the existence of a BOT-specific TF was still hypothetical. The publication of the complete *de novo* assembly of the WT strain B05.10 allowed us to identify a putative $Zn(II)_2Cys_6$ TF-encoding gene located adjacent to known *Bcbot* genes. In this study, we aimed to functionally characterize this gene and to investigate its presumed regulatory role on the BOT gene cluster. Through gene inactivation, the function of BcBot6 as a positive regulator of BOT production was examined. Moreover, we explored the genomic region containing *Bcbot* genes for A + T-rich regions/islands and the presence of RIPed TEs. Finally, we questioned the role of BOT in fungal development, virulence and response to abiotic stresses through a combination of genetic and molecular approaches.

## 2. Material and methods

### 2.1. Cultivation of B. cinerea strains

The *Botrytis cinerea* Pers.: Fr. model strain B05.10 was used as a recipient strain for genetic modifications (Quidde et al., 1998). Routine cultivation of the strains was carried out on rich medium (RM; 20 g/L malt extract, 5 g/L yeast extract and 15 g/L agar) supplemented, for mutant strains, with hygromycin B (Sigma-Aldrich; 100 μg/ml) or nourseothricin (Werner Bioagents; 80 μg/

mL). The plates were incubated in an environmental chamber at 21 °C with an alternation of 12 h of white light and 12 h of darkness. Minimal medium (MM; 20 g/L glucose, 2 g/L $NaNO_3$, 15 g/L agar, 1 g/L $KH_2PO_4$, 0.5 g/L KCl, 0.5 g/L $MgSO_4$, $7H_2O$, 0.01 g/L $FeSO_4$, $7H_2O$) and grape juice medium (pH adjusted to 4; 15 g/L agar) were also used for specific purposes. In the modified MM with ammonium, $(NH_4)_2SO_4$ at 12.5 mM was used instead of $NaNO_3$. For the expression assays, pre-cultures were grown for 8 days on RM. Then, 300 µl of a $10^6$ conidia/ml suspension were spread onto the indicated medium. The samples were collected after the required growth period. The alternation of white light and darkness was conducted in a Sanyo MLR-350H environmental chamber with fluorescent tubes OSRAM L 36 W/640.

### 2.2. Bioinformatics

The gapless genome of the strain B05.10 is available at the EnsemblFungi database (van Kan et al., 2016) (Genbank CP009805.1 to CP009822.1). The isochore-like structure of each chromosome was determined by the GC-profile software (Gao and Zhang, 2006) with parameters for detecting isochores in eukaryotic genomes, *i.e.* minimum length = 3000 bp, halting parameter = 100, gap size < 1% of the chromosome size.

Transposons were searched in the genome sequence using the previously described REPET package (http://urgi.versailles.inra.fr/tools/REPET;Amselem et al., 2015). The TEdenovo pipeline (Flutre et al., 2011) was used to detect repeated elements in the genome and to provide a consensus sequence for each family. In the first step, Blaster was used with the following parameters: identity >90%, HSPs (High Scoring segments Pairs) length >100b and <20 Kb, e-value $\leqslant$ 1e−300. Found HSPs were clustered with three different methods: Piler (Edgar and Myers, 2005), Grouper (Quesneville et al., 2005) and Recon (Bao and Eddy, 2002). For each cluster of sequences, a consensus was generated using multiple alignments of the 3–20 longest members. Consensus sequences were then classified according to their structure and similarities with the Repbase Update (v20.05; Jurka et al., 2005), rRNA_Eukaryota.fsa and Pfam27.0_GypsyDB.hmm. Consensus sequences without any known structure or similarity were classified as "noCat" and those noCat consensus built from less than ten HSPs were eliminated. Consensus sequences classified as simple sequence repeats (SSR *e.g.* micro/mini-satellites) or containing more than 30% of SSR were also eliminated. The resulting library of consensus sequences was used to annotate TE copies in the whole genome using the TEannot pipeline (Quesneville et al., 2005). In addition, a "long join procedure" (Flutre et al., 2011) was used to address the problem of nested TEs *i.e.* TEs interrupted by other TEs that were inserted more recently. Alignment between the TE detected in the BOT gene cluster and its corresponding TE consensus (DXX-MITE_P15.8) was used to estimate the transition/transversion rate and the RIP mutations, using RIPCAL (Hane and Oliver, 2008). All possible RIP mutations (CA → TA, CT → TT, CC → TC, CG → TG and their reverse complements) were computed. RIP indices were estimated on the chromosome 12 (BCIN12) from genomic position 2205751 to 2248650. RIP indices were analyzed in sliding windows of 500 nt, with 400 nt shifts, for both CA → TA and CT → TT conversions, and their reverse complement TG → TA and AG → AA respectively, by: RIP_CA = TA/(CA + TG) and RIP_CT = (TT + AA)/(CT + AG), according to (Hane and Oliver, 2008). The G + C percentage was calculated on the same sliding windows.

The nuclear localization signal (NLS) and nuclear export signal (NES) of the BcBot6 protein were respectively predicted with WOLF pSORT (http://www.genscript.com/wolf-psort.html) and NetNES 1.1 (http://www.cbs.dtu.dk/services/NetNES/) using the Bcin12g06420 protein sequence. The $Zn(II)_2Cys_6$ domain was predicted using InterPro (http://www.ebi.ac.uk/interpro/).

The updated functional data regarding the BOT gene cluster were deposited at the Minimum Information about a Biosynthetic Gene cluster (MIBiG) repository with the reference BGC0000631 (http://mibig.secondarymetabolites.org/; Medema et al., 2015).

### 2.3. Standard molecular methods

All primers used in this study are listed in Table S1. Fungal genomic DNA was prepared using a Sarcosyl-based protocol as in Dalmais et al. (2011). For diagnostic PCR reactions, the Mytaq polymerase (Bioline) was used according to the manufacturer recommendations and the high fidelity Accuzyme polymerase (Bioline) was used for cloning purposes. For Southern blot analysis of the *Bcbot6* related mutants and the screening of the *Bcbot2* gene among *Botrytis* species, genomic DNAs were digested with the restriction enzyme ClaI, and EcoRI, respectively. Then, genomic fragments were separated on 0.8% (wt/vol) agarose gel and transferred to Biodyne B (Positive) TM membrane (MPbio). Blot hybridization was performed using the DIG DNA labelling and detection kit by Roche according to the manufacturer's instructions.

### 2.4. Construction of mutant strains

All designed constructs are presented in Fig. S1. For inactivation of *Bcbot6* (Bcin12g06420), the 5′ (0.960 kb) and 3′ (0.364 kb) flanking non coding regions of the gene were amplified using the primers AP112 and AP113 and AP114 and AP115, respectively. Those constructs were then assembled with the hygromycin B resistance (*hph*) cassette (*PtrpC*::*hph*, amplified (1047 bp) with primers hphF and hphR using pCSN44 as template) and EcoRI/XhoI digested pRS426 by yeast recombinational cloning thanks to overlapping tails on the primers. The pRS426 and pCSN44 plasmids, and the yeast strain FY834 were obtained from the Fungal Genetics Stock Center (http://www.fgsc.net/gpkit.html; Colot et al., 2006). Two fragments were amplified from the yielded plasmids using AP112 and Hygro 8-5′ primers (amplifying the non-coding 5′ region of *Bcbot6* and the first part of the cassette) and AP115 and Hygro 7-3′ primers (amplifying the non-coding 3′ part of *Bcbot6* and the second part of the cassette), purified and used to transform protoplasts of the *B. cinerea* strain B05.10 (Levis et al., 1997) by the split marker technique (Fairhead et al., 1996; Catlett et al., 2003). The integration of the cassette was checked on hygromycin resistant individuals using AP117 (in the non-coding 3′ part of *Bcbot6*, outside of the used homologous region) and hygrofinU (inside of the cassette, in *PtrpC*) primers. A single round of monospore isolation was necessary to obtain homokaryotic transformants (verified using AP117 and AP118 (inside of the *Bcbot6* ORF) primers). Two homokarotic mutants were selected to confirm the integration of a single copy of the resistance cassette at the targeted locus by Southern blot analysis using a hph-designed probe (using hphR and hygro 8-5′ primers). The *ΔBcbot6 71.3* was chosen to be complemented with the integration of *Bcbot6* both at the native gene locus (*in loco*) and at the nitrate reductase *BcniaD* locus. The vector $p^{c}\Delta Bcbot6^{CIL}$ was generated in yeast by cotransformation of four PCR products (AP112/AP172, AP173/AP174, AP Nat1 pNDN F/AP Nat1 pNDN R and AP175/AP176) and EcoRI/XhoI digested pRS426 allowing to construct a DNA fragment containing the non-coding 5′ region of *Bcbot6*, the *Bcbot6* ORF, the first part of non-coding 3′ region of *Bcbot6*, the nourseothricin resistance cassette of pNDN-OGG (Schumacher, 2012) and the second part of the non-coding 3′ part of *Bcbot6*. The correct assembly of the complementation cassette was checked by PCR reactions (BcniaD 5′ sF1/AP118, AP137/AP136) and by sequencing (using primers AP120, AP158,

AP132 and hygrofinU). The vector $p^{c}\Delta Bcbot6^{niaD}$ was generated in yeast by co-transformation by two PCR products (AP177/AP173 and AP172/AP178) and SpeI/BglII digested pNDN-OGG (Schumacher, 2012) resulting in a DNA fragment containing the non-coding 5′ region of *BcniaD*, the non-coding 3′ region of *Bcbot6*, the non-coding 5′ region of *Bcbot6*, the nourseothricin resistance cassette (*PoliC::nat1*) and the non-coding 3′ part of *BcniaD*. The correct assembly of the complementation cassette targeting the *BcniaD* locus was verified by PCR reactions (AP118/Nat1 hiF and hygrofinU/pRS426short 3R) and by sequencing (using primers pRS426 short 5F, AP132, AP137, AP158 ad AP120). Both vectors $p^{c}\Delta Bcbot6^{CIL}$ and $p^{c}\Delta Bcbot6^{niaD}$ were digested by PvuII (ThermoFisher Scientific) which cuts on both sides of each complementation cassette. Those digestion products were used to transform protoplasts of *B. cinerea ΔBcbot6 71.3*. Nourseothricin-resistant transformants were analyzed by PCR for integration at the targeted loci (AP118/AP25 for the *BcniaD* locus and AP117/AP118 for the *Bcbot6* locus).

To be able to localize the BcBot6 protein, the gene was put under the control of a constitutive promoter (*PoliC*) and fused to the green fluorescent protein (GFP) in C terminal position. In order to construct the vector $p^{c}\Delta Bcbot6^{GFP}$, the *Bcbot6* ORF was amplified using AP154/AP155 primers (which overlap respectively *PoliC* and *gfp*) of the pNDN-OGG (Schumacher, 2012). The PCR product was co-transformed in yeast with NcoI-digested pNDN-OGG. The total insert was amplified by PCR using pRS426short 5F/pRS426short 3R primers and was used to transform protoplasts of *ΔBcbot6 71.3*. The insertion of the construct at the targeted locus was verified by diagnostic PCR using AP25/AP27 primers.

### 2.5. qRT-PCR analyses

Cultures of the WT strain B05.10, *ΔBcbot6* and complemented strains were used to prepare DNA-free RNA. cDNA were obtained from 1 µg of total RNA by a retro-transcription step realized with the M-MLV (Invitrogen) reverse transcriptase according to the manufacturer's suggestions except that both oligo(dT) (25 ng/µl) and random primers (25 ng/µl) were used. The RT-qPCR reactions were performed on 1:10 diluted cDNA using MESA Green qPCR Mastermix Plus for SYBR Assay (Eurogentec) and the CFX96 Touch real-time PCR detection system (Bio-Rad). The oligonucleotide primers used (200 nM each) to quantify the transcription level of the genes are listed in Table S1. "No Reverse Transcription" (NRT) controls were performed once on cDNA samples and "No Template Control" (NTC) were made for each pair of primers in every run. The qRT-PCR program consisted in a preliminary 5 min denaturation step at 95 °C followed by 40 amplification cycles of 15 s of denaturation (95 °C) and 1 min of annealing/extension (60 °C). Analysis of the melting curves (increment of 0.1 °C/min) of the final PCR products indicated the absence of contaminations and primer dimers. The data were analyzed with the CFX manager software. Efficiency reactions of the pairs of primers were tested once on the cDNA sample and were all superior to 90%. Gene expression levels were calculated as the ratio between the gene of interest (GOI) and the *BcactA* reference gene or following the $2^{-\Delta\Delta CT}$ method (Livak and Schmittgen, 2001).

### 2.6. Localization study

For detection of nuclei, nucleic acids were stained using the fluorescent dye Hoechst 33342 (Sigma). In brief, 10 µl of an Hoechst solution was freshly prepared according to (Kangatharalingam and Ferguson, 1984) and was added to germinated conidia prior to microscopic observations. Confocal images were acquired on a TCS SPE inverted confocal laser scanning microscope (Leica Microsystems) with a 63× (NA 1.30) ACS APO objective Leica. Differential interference microscopy (DIC) was used for bright field images when indicated. GFP fluorescence was captured by excitation at 488 nm and emission in the range 493–559 nm; Hoechst 33342 fluorescence was captured by excitation at 40 nm and emission in the range 422–478 nm. All images were acquired at 0.4 Hz and the power output of the laser adjusted to ensure sufficient fluorophore excitation with no saturation of the emission signal. To avoid fluorescent bleed-through, images were acquired sequentially whereby the acquisition bandpass was set as far from each other as possible. Images were analyzed using the Leica Application Software package (LAS-AF v3.1.3 build 8976) and edited with the FigureJ plugin of the ImageJ software (Mutterer and Zinck, 2013).

### 2.7. Analysis of metabolite production

For analysis of metabolite production, strains were grown on malt agar medium (MA; 20 g/L D-glucose, 10 g/L malt extract, 20 g/L agar, 1 g/L peptone, pH 6.5–7) at 25 °C. Ten 150 mm diameter-Petri dishes containing 100 ml of MA were inoculated with three 4 mm diameter-mycelial plugs each and incubated for either 5 days or 12 days at 25 °C. Then MA was extracted with ethyl acetate (3 × 0.5 vol.) using an ultrasonic bath, 30 min. The organic extracts were dried over $Na_2SO_4$ and concentrated to dryness to yield dark oil extracts.

$^{1}H$ and $^{13}C$ Nuclear Magnetic Resonance (NMR) measurements on metabolites isolated from culture extracts were obtained on Agilent 400-MR NMR and Agilent 500 MHz NMR spectrometers with $SiMe_4$ as the internal reference. High-pressure liquid chromatography (HPLC) was performed with a Hitachi/Merck L-6270 apparatus equipped with a UV–vis detector (L 6200) and a differential refractometer detector (RI-71). Thin Layer Chromatography (TLC) was performed on Merck Kiesegel 60 $F_{254}$, 0.2 mm thick. Silica gel (Merck) was used for column chromatography. HPLC purification was accomplished with a silica gel column (Hibar 60, 7 m, 1 cm wide, 25 cm long). Chemicals were products of Fluka or Aldrich. All solvents were freshly distilled.

For metabolites isolation and characterization, the dark oil extracts obtained from fermentation experiments of *B. cinerea* strains were separated by means of column chromatography on silica gel, with a mixture of ethyl acetate/hexane (10, 20, 40, 60, 80 and 100% ethyl acetate), and 20% methanol in ethyl acetate as solvent.

Extensive spectroscopic analysis by $^{1}H$-NMR and $^{13}C$-NMR were used to detect the presence of the various toxins in each fraction. Candidate fractions were further purified by HPLC with an increasing gradient of ethyl acetate to petroleum ether. The toxin structures were analyzed by spectroscopic methods and direct comparison with authentic samples previously isolated from strains of *B. cinerea* (Collado and Viaud, 2016). Semi-preparative HPLC afforded the quantification of the metabolites.

## 3. Results

### 3.1. The botrydial biosynthetic gene cluster is nested between stretches of A + T-rich sequences containing relics of transposable elements

Previously, the BOT gene cluster was described as five co-regulated genes that encode the enzymes required for the synthesis of the toxin *i.e.* the key sesquiterpene cyclase (BcBot2), three P450 mono-oxygenases (BcBot1, 3 and 4) and a putative acetyl transferase (BcBot5) (Fig. 1A, Table 1) (Siewers et al., 2005; Pinedo et al., 2008; Moraga et al., 2016). In those previous studies, A + T-rich regions upstream from *Bcbot4* and downstream from *Bcbot5* led to cloning and sequencing issues and prevented the

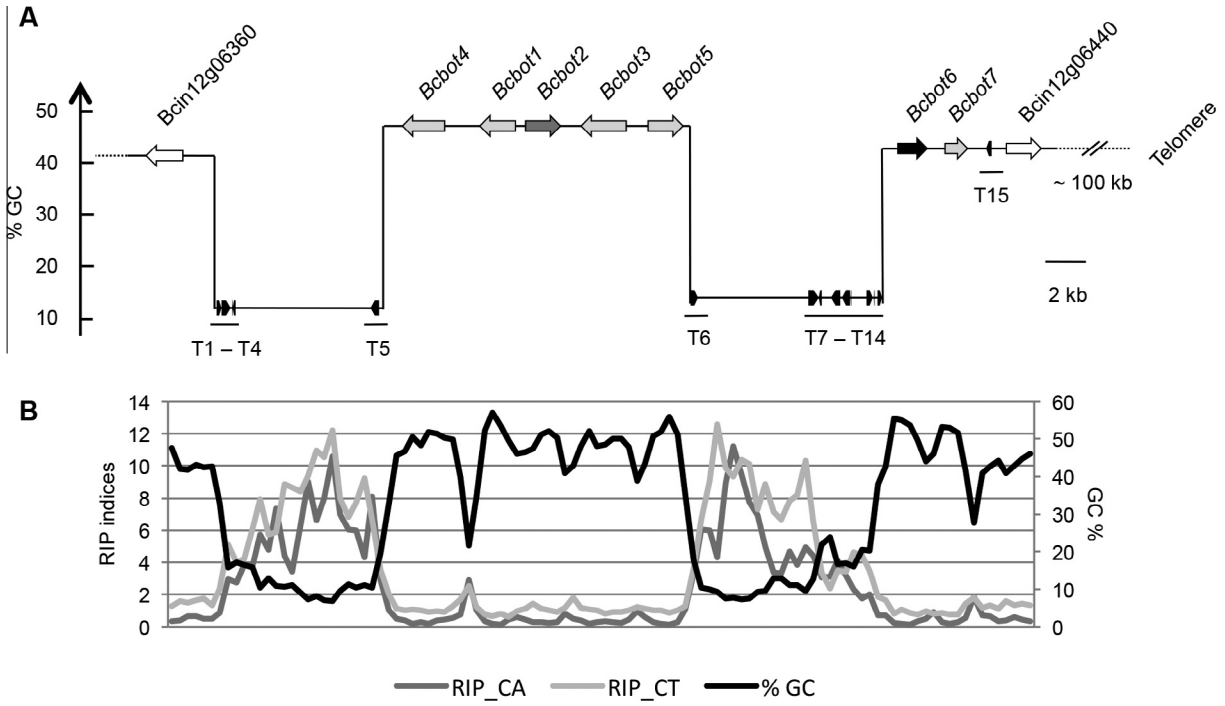


**Fig. 1.** The botrydial (BOT) gene cluster in the *Botrytis cinerea* strain B05.10 is located in a bipartite genomic region containing A + T-rich sequences mutated by RIP. (A) The BOT gene cluster was assigned to the chromosome 12 of the strain B05.10 (van Kan et al., 2016) which allowed to detect the genes located upstream and downstream from the five previously identified *Bcbot* genes (Pinedo et al., 2008). Transposable elements (TEs) were identified using the REPET package (http://urgi.versailles.inra.fr/tools/REPET; Amselem et al., 2015) (see details in Table 1). Variations in G + C content were computed with GC-profile (Gao and Zhang, 2006), allowing the identification of four segmentation points in the BOT cluster. (B) G + C percent and RIP indices were analyzed in 500 nt windows, with 400 nt shifts over the BOT cluster genomic sequence. RIP_CA and RIP_CT represent the ratio of conversion of pre-RIP di-nucleotides to post-RIP dinucleotides CA → TA or CT → TT respectively, and their corresponding reverse complement TG → TA or AG → AA.

**Table 1**
Genes and copies of transposable elements (TEs) located in the genomic environment of the botrydial gene cluster.

| Gene/TE copy | Gene/TE consensus name | Length (bp) | Gene function |
|---|---|---|---|
| | Bcin12g06350 | 1, 912 | Putative sugar transporter |
| | Bcin12g06360 | 1811 | Putative carboxylesterase |
| *T1* | noCat_G9 | 233 | |
| *T2* | DXX-MITE_P15.8 | 452 | |
| *T3* | noCat_G9 | 43 | |
| *T4* | DXX-MITE_P15.8 | 164 | |
| *T5* | noCat_G9 | 413 | |
| *Bcbot4* | Bcin12g06370 | 2100 | Monooxygenase (Moraga et al., 2016) |
| *Bcbot1* | Bcin12g06380 | 1754 | Monooxygenase (Siewers et al., 2005) |
| *Bcbot2* | Bcin12g06390 | 1721 | Sesquiterpene cyclase (Pinedo et al., 2008) |
| *Bcbot3* | Bcin12g06400 | 2245 | Monooxygenase(Moraga et al., 2016) |
| *Bcbot5* | Bcin12g06410 | 1735 | Putative acetyl transferase |
| *T6* | noCat_G9 | 365 | |
| *T7* | noCat_G9 | 521 | |
| *T8* | DXX-MITE_P15.8 | 139 | |
| *T9* | noCat_G9 | 436 | |
| *T10* | noCat_G9 | 384 | |
| *T11* | DXX-MITE_G19 | 36 | |
| *T12* | DXX-MITE_P15.8 | 295 | |
| *T13* | DXX-MITE_P15.8 | 25 | |
| *T14* | RLX_P13.1 | 195 | |
| *Bcbot6* | Bcin12g06420 | 1455 | $Zn(II)_2Cys_6$ transcription factor |
| *Bcbot7* | Bcin12g06430 | 1119 | Putative dehydrogenase |
| *T15* | RLX_P26.1 | 257 | |
| | Bcin12g06440 | 1712 | Putative DNA methylase |

Genes and TE copies are listed in the order they appear on BCIN12 chromosome (see Fig. 1A). The TE consensus names refer to the consensus names listed in Table 2.

identification of neighboring genes. Recently, the genome of the wild type (WT) strain B05.10 was sequenced with the PacBio technology which resulted in a gapless sequence of the sixteen core and two dispensable chromosomes (van Kan et al., 2016). Thanks to this new genome release, the BOT gene cluster was assigned to the core chromosome 12 (BCIN12, 2.3 Mb) at approximately 100 kb from the telomere and the structure of the surrounding genomic region was characterized.

The analysis of G + C content (Fig. 1B) highlights the presence of gene-depleted A + T-rich regions on both sides of the BOT cluster. By contrast, the G + C content of the *Bcbot1-Bcbot5* locus and the upstream and downstream gene-containing regions are similar to the overall G + C content of the B05.10 genome (42.75%; Staats and van Kan, 2012). To better visualize and analyze the bipartite structure of this genomic region, we computed the segmentation points on *B. cinerea* chromosomes using the GC-profile webtool (http://tubic.tju.edu.cn/GC-Profile/ Gao and Zhang, 2006). Nineteen segmentation points were identified on BCIN12. Four of them are located around the BOT gene cluster (Fig. 1A), coinciding with the boundaries of A + T-rich regions and thereby confirming the observation of a difference in G + C composition between gene-containing and gene-depleted genomic regions. Particularly, the area containing *Bcbot1-Bcbot5* genes is 47.26% G + C-rich whereas upstream and downstream gene-less regions only contain 11.86 and 13.09% of G + C, respectively. In many fungi including *B. cinerea*, it is well documented that A + T-rich regions may result from a pre-meiotic genome defense mechanism named Repeat-Induced Point mutation (RIP) that silences repeated sequences by mutating C to T consequently increasing the A + T content (Amselem et al., 2015; Hane et al., 2015). We thereby tested the hypothesis that the presence of A + T-rich regions surrounding the BOT gene cluster might originate from transposable elements

(TEs) that would have been silenced by RIP. We used the gapless genomic sequence of B05.10 (van Kan et al., 2016) and undertook the complete annotation of the TEs using the previously described REPET package (Flutre et al., 2011; Amselem et al., 2015). Fifteen consensus sequences representing all the possible TEs among the genome were identified. Each consensus sequence had at least one full-length copy in the genome as well as many incomplete copies. The consensus sequences were classified according to their structure and sequence similarities to characterized eukaryotic transposons (Wicker et al., 2007; Hoede et al., 2014). This classification (Table 2) indicates that the genome of the strain B05.10 contains nine different LTR (Long Terminal Repeats) retrotransposons, four DNA transposons and two unknown repeated elements. Altogether, the TE copies cover 3.72% of the genome. With regards to the BOT gene cluster area, fifteen copies (T1–T15) corresponding to two DNA transposons, two retrotransposons and one unknown repeated element were predicted (Fig. 1A, Table 1). As expected, these copies are located in the A + T-rich regions except T15 that is present within a G + C/A + T equilibrated region (between Bcin12g06430 and Bcin12g06440). The annotated TE copies are short (often less than 400 bp) and are degenerated compared to their consensus. Such TEs may correspond to copies that have undergone RIP-associated C to T mutations as previously described in *B. cinerea* (Amselem et al., 2015). To examine this hypothesis, we used two different strategies. The first one aligns each TE copy to its consensus sequence. Unfortunately, only one TE copy *i.e.* T2 was long enough (>400 nt) and harbored enough identity (>80%) with the corresponding TE consensus sequence (DXX-MITE_P15.8; Tables 1 and 2) to provide a good alignment. This allowed determining the rate of base transitions versus transversions and the number of RIP di-nucleotide mutations using RIPCAL (Hane and Oliver, 2008). The ratio transitions/transversions equaled 5.5, strongly suggesting the occurrence of RIP. Furthermore, all possible RIP induced mutations (CA → TA, CT → TT, CC → TC, CG → TG and their reverse complements) were computed. The results indicated that the RIP mutation at the dinucleotide CA → TA (and reversibly TG → TA) represents 46.4% of all the detected RIP mutations, whereas the CT → TT, CC → TC and CG → TG mutations represent 21.4%, 14.3% and 17.9% respectively. These predominant CA and CT dinucleotide signatures, consistent with previous analysis in *B. cinerea* (Amselem et al., 2015), strongly suggest that this TE copy was submitted to RIP. Alternatively, an overall strategy was performed on the whole BOT genomic region. RIP indices were computed to determine the likely C to T mutation in CA and CT dinucleotides, according to (Hane and Oliver, 2008). The results (Fig. 1B) showed that CA and CT RIP indices massively increased in both A + T-rich regions, suggesting that RIP may have occurred in these regions. On the other hand, RIP indices were low in G + C/A + T equilibrated regions demonstrating no RIP action. An intermediate profile was observed at the T15 locus where G + C content drops to less than 30% and where RIP indices are slightly increased. Interestingly, the same profile was observed in the *Bcbot4* promoter region (Fig. 1).

### 3.2. BcBot6 regulates the Bcbot genes

Genomic regions upstream and downstream from the known *Bcbot1-Bcbot5* cluster were investigated in order to search for a gene encoding a regulator of BOT synthesis as well as possible additional genes that might be involved in the biosynthesis and transport of the toxin (Fig. 1A). Interestingly, the two genes located downstream from the 10 kb A + T-rich stretch adjacent to *Bcbot5* belong to families often found in fungal SM gene clusters: Bcin12g06420 was predicted to encode a $Zn(II)_2Cys_6$ TF (IPR001138) whereas Bcin12g06430 was predicted to encode a dehydrogenase (IPR002198, IPR016040 and IPR002347) that might be involved in the conversion of BOT to dihydrobotrydial (Siewers et al., 2005; Collado and Viaud, 2016). These two genes were thereafter named *Bcbot6* and *Bcbot7*, respectively. The gene located downstream from *Bcbot7*, Bcin12g06440, encodes a DNA methylase (IPR002052, IPR029063 and IPR007757) that is likely not part of the studied cluster. Similarly, the gene located upstream from the A + T-rich stretch adjacent to *Bcbot4*, Bcin12g06360, encodes a predicted carboxylesterase (IPR002018, IPR029058 and IPR019819) whose function is probably unrelated to BOT biosynthesis.

To specify the borders of the BOT gene cluster, we further considered available microarrays transcriptomic data sets (Fig. S2). Gene expression during infection of grape berries (Kelloniemi et al., 2015) and in the *ΔBcve1*, *ΔBclae1* and *ΔBcyoh1* mutants (Schumacher et al., 2015; Simon et al., 2013) suggests that the *Bcbot1-Bcbot7* genes are co-regulated while the surrounding genes have different expression profiles. Finally, orthology analysis (Fig. S2 D) indicated that the *Bcbot*1 to *Bcbot7* genes do not have any ortholog in the closely related species *Sclerotinia sclerotiorum* (Amselem et al., 2011) while the adjacent genes Bcin12g06360 and Bcin12g06440 have co-localized orthologs in the genome of *S. sclerotinium (SSIG_13881 and SSIG_13879).* Both expression and synteny data therefore suggest that the BOT gene cluster is restricted to *Bcbot1* to *Bcbot7* genes.

In general, fungal SM gene clusters contain a gene encoding a Zn $(II)_2Cys_6$ TF that specifically regulates the genes of the cluster (Brakhage, 2012; Knox and Keller, 2015). As the protein encoded by *Bcbot6* displays this DNA-binding domain (IPR001138), we hypothesized that it might be a specific regulator of the BOT gene cluster even though the gene is separated from the *Bcbot5* gene by a 10 kb-long A + T-rich stretch.

To characterize the role of BcBot6, we generated knock out mutants in which the whole ORF of *Bcbot6* was replaced by the hygromycin-resistance *hph* gene (Fig. S1). Two homokaryotic transformants (*ΔBcbot6 41.1* and *71.3*) were selected for this study. To confirm the results obtained with the two mutants, complemented strains were constructed by reintroducing the ORF as well as the 0.729 kb non-coding 5′ part and 0.366 kb non-coding 3′ part of *Bcbot6* both at the native locus ($^{c}\Delta Bcbot6^{CIL}$; CIL: complementation *in loco*) and at the nitrate reductase-encoding gene *BcniaD* locus ($^{c}\Delta Bcbot6^{niaD}$) using of the *ΔBcbot6 71.3* as background strain.

To study the implication of BcBot6 in the regulation of the *Bcbot* genes, qRT-PCR were carried out. The expression of the *Bcbot* genes was monitored in the two independent KO mutants *ΔBcbot6 41.1* and *71.3* as well as in the WT strain B05.10 (Fig. 2A). Moreover, the expression of the two putative flanking genes (Bcin12g06360 and Bcin12g06440) as well as the putative sugar transporter-encoding gene Bcin12g06350 was also studied. The results showed that all the *Bcbot* genes were significantly under-expressed in both *ΔBcbot6* mutants. The key enzyme encoding-gene *Bcbot2* was about 1000 times less expressed than in the WT strain. The neighbor gene *Bcbot1*, putatively sharing a bidirectional promoter region with *Bcbot2*, exhibited a similar decrease with an expression level 500 times lower than in the WT. *Bcbot3* and *Bcbot5*, also putatively sharing a common promoter region, were around 100 and 200 less expressed than in the WT. Finally, *Bcbot4* and *Bcbot7* were ten times less expressed than in the WT. By contrast, the expression of Bcin12g06350, Bcin12g06360 and Bcin12g06440 exhibited no significant difference between mutants and B05.10. Overall, the expression patterns indicated that the *Bcbot1* to *Bcbot5* genes as well as the newly identified *Bcbot7* gene are dependent on the BcBot6 protein. These data further support our supposition that the BOT gene cluster is indeed composed of *Bcbot1* to *Bcbot7* and that Bcin12g06350, Bcin12g06360 and Bcin12g06440 are not part of the cluster.

**Table 2**
Transposable elements (TEs) identified in the genome of *Botrytis cinerea* strain B05.10.

| Repeated element | Consensus name (*B. cinereaTE name*) | Number of copies | Genome coverage (%) | Copies length (bp) |
|---|---|---|---|---|
| **Class I LTR** | | **554** | **2.34** | **21–10,980** |
| | RLX_ P17.7 | 32 | 0.14 | 30–6459 |
| | RLX_P21.1 (*Boty*) | 76 | 0.43 | 57–6699 |
| | RLX_P26.1 (*Boty*) | 81 | 0.27 | 27–6649 |
| | RLX_P6.1 (*Boty*) | 34 | 0.14 | 50–6437 |
| | RLX_B-R56 | 43 | 0.28 | 21–7402 |
| | RLX_G54 | 25 | 0.14 | 32–8277 |
| | RLX_G57 | 164 | 0.57 | 24–10,980 |
| | RLX_P13.1 (*Boty*) | 35 | 0.12 | 21–6578 |
| | RLX_P27.0 | 64 | 0.25 | 21–6405 |
| **Class II TIRE** | | **72** | **0.15** | **27–1880** |
| | DTX_G36 | 31 | 0.09 | 31–1880 |
| | DTX_P14.9 (*Flipper*) | 41 | 0.06 | 27–1855 |
| **Class II MITE** | | **788** | **0.51** | **22–849** |
| | DXX-MITE_G19 | 63 | 0.04 | 36–497 |
| | DXX-MITE_P15.8 | 725 | 0.47 | 22–849 |
| **Unknown** | | **513** | **0.72** | **26–13,266** |
| | noCat_G9 | 460 | 0.44 | 26–639 |
| | noCat_R20 | 53 | 0.27 | 34–13,266 |
| **Total** | | **1927** | **3.72** | **21–13,266** |

The new gapless genome sequence (van Kan et al., 2016) was analyzed with the REPET package (http://urgi.versailles.inra.fr/tools/REPET). The fifteen consensus sequences were classified according to (Wicker et al., 2007). The sequence of the consensus sequences (BCINB05_10_18Chr_RefTE.fa) as well as their annotation file (BCINB05_10_18Chr_RefTE_annotation.gff3) are available at https://urgi.versailles.inra.fr/download/fungi/TEs/.

To confirm that the down-regulation of the BOT gene cluster is due to the inactivation of the *Bcbot6* gene, the expression of *Bcbot6* as well as the key enzyme-encoding gene *Bcbot2* was monitored in the complemented strains $^{c}\Delta Bcbot6^{CIL}$ and $^{c}\Delta Bcbot6^{niaD}$ (Fig. S3). The expression of both genes was restored reaching an expression level similar to B05.10 when *Bcbot6* was reintroduced in the mutant background regardless whether the reinsertion occurred at the native (mutated) locus or in the *BcniaD* locus.

To determine if BcBot6 might have a role in the regulation of other SM gene clusters, we performed, as above, expression assays using qRT-PCR on genes belonging to different SM gene clusters that were also shown to be expressed during infection and to be regulated through the Velvet complex (reviewed in Viaud et al., 2016). The first gene tested was *Bcboa6* (Bcin01g00060) that encodes a PKS involved in the production of BOA (Dalmais et al., 2011) and whose expression is positively regulated by both BcVel1 and BcLae1 (Schumacher et al., 2015). The second gene tested encodes a PKS with additional non-ribosomal peptide synthetase (NRPS) domains (*Bcpks7*; Bcin10g00040) and belongs to a SM gene cluster that is positively regulated by BcVel1 during infection (Schumacher et al., 2012). The results in Fig. 2B were consistent with the previous ones for *Bcbot2* expression. The expression in the WT was about twice as high as the actin encoding gene and dramatically decreased in both *ΔBcbot6* mutants. However, for *Bcboa6* and *Bcpks7*, no significant difference was observed between B05.10 and the mutants, indicating that the *Bcboa6* and *Bcpks7* genes are not regulated by BcBot6. In sum, the results suggest that BcBot6 is the main positive regulator of the BOT gene cluster. As neither *Bcboa6* nor *Bcpks7* expression is affected by the deletion of the *Bcbot6* gene, we hypothesize that this TF is a BOT pathway specific regulator.

### 3.3. The deletion of Bcbot6 suppresses the production of botrydial and other botryanes

To support findings from the expression assays presented above, botryanes and botcinins produced by the WT strain B05.10 and the different mutants were investigated (Fig. S4, Tables 3 and S2). As botryanes and botcinins are known to reach their maximum amount after five and twelve days of fermentation, respectively (Durán-Patrón et al., 2004; Collado et al., unpublished), these two time points were chosen to investigate their production. Toxins were isolated by column chromatography and analyzed by HPLC as well as $^{1}H$ and $^{13}C$ NMR.

As expected from previous studies, the WT strain B05.10 produced significant amounts of botryanes (Fig. S4 (**1**–**6**), Tables 3 and S2), *i.e.* 9.1% of the total extract, after 5 days of cultures whereas the *ΔBcbot6 71.3* did not produce any botryanes even after 12 days of culture. In addition, in the complemented transformants $^{c}\Delta Bcbot6^{niaD}$, $^{c}\Delta Bcbot6^{CIL}$ and $^{c}\Delta Bcbot6^{GFP}$ the production of botryanes was restored demonstrating that BcBot6 is required for the activation of the BOT biosynthesis pathway.

Quantification of botcinins (Fig. S4 (**7**–**8**), Tables 3 and S2) also highlighted differences between the studied strains. After 12 days of culture, the *ΔBcbot6 71.3* accumulated significantly higher quantities of these polyketides compared to the WT strain (5.4% instead of 2.7% of the total extract). In the three complemented strains, $^{c}\Delta Bcbot6^{niaD}$, $^{c}\Delta Bcbot6^{CIL}$ and $^{c}\Delta Bcbot6^{GFP}$, the production of botcinins was similar to those of the WT strain B05.10. This overproduction of botcinins in the absence of botryanes was previously observed with the deletion of the key enzyme-encoding gene *Bcbot2* (Pinedo et al., 2008).

### 3.4. BcBot6 is a nuclear protein

BcBot6 is a 484 aa protein that in addition to the N-terminal Zn $(II)_2Cys_6$ domain displays two nuclear localization signal (NLS) and one nuclear export signal (NES) (Fig. 3A). To study the cellular localization of BcBot6 in living hyphae, we transformed the *ΔBcbot6 71.3* with a cassette containing *Bcbot6* under the control of a constitutive promoter *PoliC* and fused to the codon-optimized GFP (Fig. S1; Leroch et al., 2011). The functionality of the BcBot6-GFP hybrid protein in the resulting strain ($^{c}\Delta Bcbot6^{GFP}$) was verified by both expression analysis and metabolic studies. The expression of the key enzyme-encoding gene *Bcbot2* (data not shown) as well as the production of botryanes (Tables 3 and S2) were restored in the complemented mutant $^{c}\Delta Bcbot6^{GFP}$. The confocal microscopy observations presented in Fig. 3B highlight

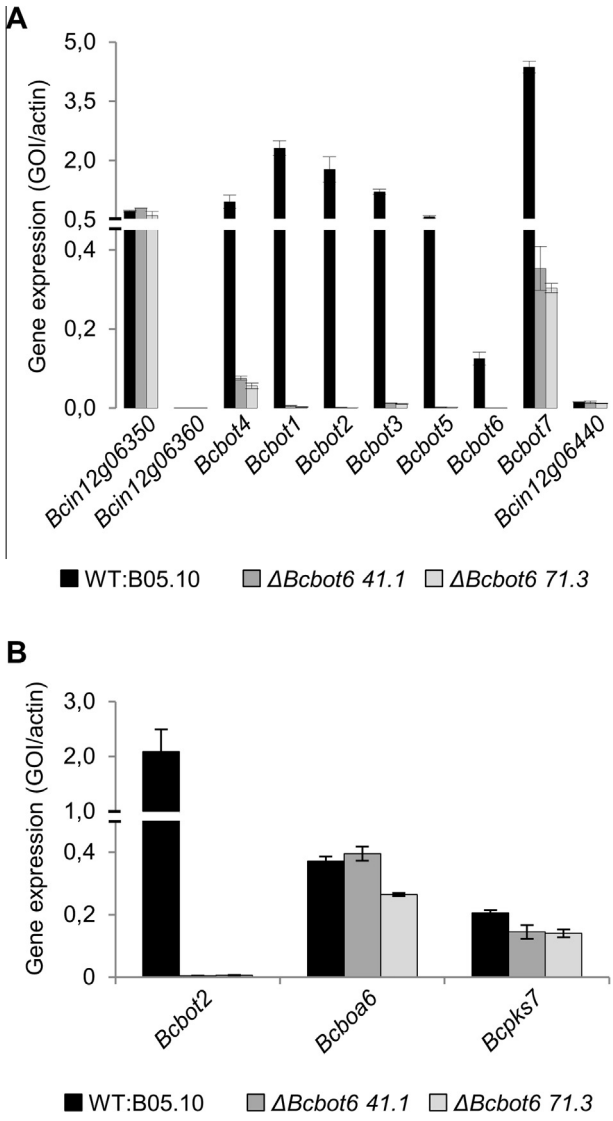


**Fig. 2.** The putative $Zn(II)_2Cys_6$ TF BcBot6 positively regulates the botrydial (BOT) gene cluster. (A) The expression of *Bcbot1-BcBot7*, Bcin12g06350, Bcin12g06360 and Bcin12g06440 was monitored by RT-qPCR in the WT strain B05.10 and two independent *ΔBcbot6* mutants. (B) The expression of two SM key enzyme-encoding genes that are not part of the BOT cluster (*Bcboa6* (Bcin01g00060) and *Bcpks7* (Bcin10g00040)) was monitored by RT-qPCR in the WT strain B05.10 and two independent *ΔBcbot6* mutants. For all the results presented here, the strains were grown for 48 h at 23 °C on solid grape juice with a photoperiod of 14 h of darkness and 10 h of white light. Gene expression was calculated as the ratio between the gene of interest (GOI) and the reference gene *BcactA* (Bcin16g02020). Means and standard deviations were collected from two biological replicates and three technical replicates.

the co-localization of BcBot6-GFP with Hoechst stained nuclei suggesting this TF is primarily nuclear localized.

### 3.5. BcBot6 is dispensable for development, virulence and resistance to abiotic stresses in the B05.10 strain

Previously, studies of *ΔBcbot1* and *ΔBcbot2* demonstrated that the production of BOT is not necessary for either saprophytic growth or conidiation in *B. cinerea*. Moreover, BOT was shown to be a strain specific virulence factor that is dispensable in strains producing BOA *i.e.* B05.10 or SAS56 (Siewers et al., 2005; Pinedo et al., 2008; Dalmais et al., 2011). Here, the phenotype of the *ΔBcbot6* mutant was first characterized to determine whether the TF may have functions in addition to the synthesis of this toxin. Inoculation of the *ΔBcbot6* mutants on either a rich medium (RM), a synthetic minimal medium (MM) or a grape juice medium indicated that they grow and conidiate as the WT parental strain B05.10 (Fig. S5). In order to test whether illumination conditions could highlight a developmental defect, we grew the mutants on RM either in constant light, or constant darkness or in an alternating light/dark (12 h/12 h) regime. The results indicated that the mutants exhibit a light dependency similar to the WT strain *i.e.* they conidiate in the presence of light and produce sclerotia in constant darkness (Fig. S5). Finally, pathogenicity tests conducted on French bean leaves using either young mycelium plugs or conidia as inoculum (Fig. 4 and S6) showed that the mutants are as aggressive as the WT strain. In conclusion, these phenotypic data indicate that the absence of the BcBot6 regulator, similarly to the absence of one of the BOT biosynthetic enzymes (*e.g.* BcBot2; Dalmais et al., 2011), does not alter the development and virulence of the strain B05.10.

The phenotype of the *ΔBcbot6* mutants was further investigated to search for a potential role of BcBot6 in response to several abiotic stresses and two nitrogen sources. The mutants were cultivated on MM supplemented with NaCl or sorbitol to induce an osmotic stress, with hydrogen peroxide ($H_2O_2$) and menadione to induce a redox stress or with calcofluor white to induce a cell wall stress. In addition, ammonium was used as an alternative nitrogen source to nitrate in the original MM. In all tested conditions, the *ΔBcbot6* mutants exhibited a similar growth rate as the WT strain (Table S3). Altogether, these phenotypic data indicate that the BcBot6 TF is dispensable for development, virulence and tolerance to abiotic stresses in the strain B05.10.

### 3.6. The expression of the botrydial key enzyme-encoding gene Bcbot2 is regulated by the nitrogen source

To estimate whether abiotic stresses or nitrogen sources may affect the regulation of the BOT gene cluster, we investigated the expression of the key enzyme-encoding gene *Bcbot2* using the same culture conditions as above. After 96 h of growth, total RNAs

**Table 3**
Botryanes and botcinins produced by the recipient strain B05.10 and mutants after 5 and 12 days of culture.

| Strain | Metabolite production (mg $L^{-1}$ (% of total extract)) | | | | | |
|---|---|---|---|---|---|---|
| | 5 days | | | 12 days | | |
| | Total extract | Botryanes | Botcinins | Total extract | Botryanes | Botcinins |
| WT:B05.10 | 81 (100) | 7.3 (9.1) | 0.9 (1.1) | 238 (1 0 0) | 0.6 (0.3) | 6.4 (2.7) |
| *ΔBcbot6 71.3* | 149 (100) | **0 (0)** | **2.3 (1.5)** | 319.8 (1 0 0) | **0 (0)** | **17.3 (5.4)** |
| $^{c}$*ΔBcbot6$^{niaD}$* | 103.5 (100) | 12.9 (12.4) | 1.1 (1) | 261.4 (1 0 0) | 14.8 (5.7) | 5.2 (2) |
| $^{c}$*ΔBcbot6$^{CIL}$* | 115.3 (100) | 5.8 (5.1) | 1.1 (1) | 237.2 (1 0 0) | 4.7 (2) | 5.9 (2.5) |
| $^{c}$*ΔBcbot6$^{GFP}$* | 111.2 (100) | 14.2 (12.8) | 1 (0.9) | 312.3 (1 0 0) | 15.2 (4.9) | 4.7 (1.5) |

The percentage of the indicated metabolite over the total extract of the same strain is indicated in brackets.

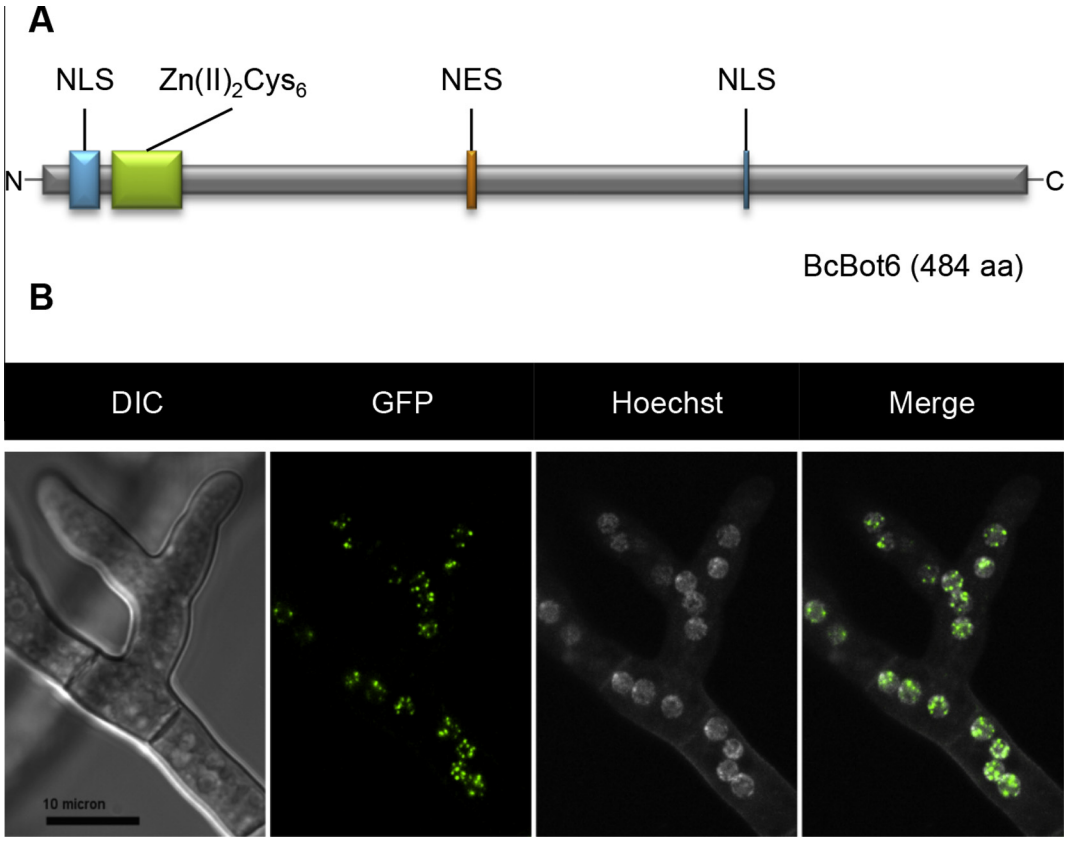


**Fig. 3.** The putative $Zn(II)_2Cys_6$ TF BcBot6 is localized into the nucleus. (A) The NLS, NES and Zn(II)2Cys6 TF domains were predicted using the whole predicted BcBot6 protein (Bcin12g06420). For more details, see *Experimental procedures*. (B) BcBot6 protein was fused to GFP and localized by fluorescence microscopy. Conidia of the strain $^{c}\Delta Bcbot6^{GFP}$ were inoculated in NY liquid medium (Malt extract 2%, Yeast extract 0.2%). and deposited on a microscope slide The observation was conducted after 16 h (10 h of white light and 6 h of darkness) at 23 °C. Nuclei were stained with Hoechst.

were extracted and processed to analyze the expression of *Bcbot2* by qRT-PCR. The synthetic MM was used as control to the representation of the results in Fig. 5. No significant difference for *Bcbot2* expression was detected when cell wall or osmotic stress are applied to the fungus. In contrast, a slight increase (2.5 fold) was observed when B05.10 was grown on medium supplemented with $H_2O_2$. A decrease (4 fold) was observed on RM and a stronger one (nearly 8 fold) was observed when the nitrogen source in MM was ammonium instead of nitrate. These results suggest that of the tested conditions, the nitrogen source is the only factor that might have an impact, either directly or indirectly, on the expression of *Bcbot2*.

### *3.7. B. fabae and B. pseudocinerea species which are closely related to B. cinerea lack a functional BOT gene cluster*

In order to examine the extent of the BOT cluster in *B. cinerea* populations but also in other *Botrytis* species, we screened a collection of 27 strains for the presence of the key enzyme-encoding gene *Bcbot2*. The results of PCR and Southern hybridizations (Table S4) showed that the *Bcbot2* gene was present in all *B. cinerea* strains tested (*i.e.* twelve) consistent with the observation that all eleven strains tested by Reino et al. (2003) produced botryanes. By contrast, the *Bcbot2* gene was absent in the closely related species *B. fabae* (five strains tested) and *B. pseudocinerea* (five strains tested) that are pathogenic toward fabaceae and polyphagous, respectively. Finally, the gene was detected in the more distant species *B. squamosa* known to produce botryanes (Collado et al., 2000) as well as in *B. aclada* and *B. porri*. These species are all pathogenic towards *Allium* species. In conclusion, our molecular data point out a patchy distribution of the BOT gene cluster in the *Botrytis* genus. Moreover, they indicate that the closely related polyphagous and sympatric species *B. cinerea* and *B. pseudocinerea* (Walker et al., 2011) differ in their ability to produce BOT.

## 4. Discussion

In this study, we demonstrated that the *B. cinerea* BcBot6 zinc finger protein, which is located adjacent to five structural genes involved in BOT biosynthesis, is dedicated to the regulation of the BOT gene cluster. The characterization of the BOT gene cluster highlighted its particular genomic environment and depicted its occurrence in the populations of the gray mold agent.

### *4.1. Botrydial biosynthesis depends on the putative pathway-specific transcription factor BcBot6*

One hallmark of fungal SM cluster genes is their co-regulation by pathway-specific TFs (Yu and Keller, 2005). Such proteins, typically harboring a $Zn(II)_2Cys_6$ TF domain, have been characterized in different fungal species (Knox and Keller, 2015). Nevertheless, the deletion of the genes encoding such regulators not always affects the expression of all the genes in the cluster. For example, the deletion of the *Fusarium fujikoroi* TF-encoding gene *bik5* significantly affected the expression of only three of the five adjacent genes belonging to the bikaverin biosynthetic gene cluster (Wiemann et al., 2009). In the present study, we aimed to investigate the putative regulatory role of BcBot6 on the *Bcbot* genes. The presence of a $Zn(II)_2Cys_6$ TF domain and the nuclear localization of the protein strongly suggest that BcBot6 is a TF. We showed that

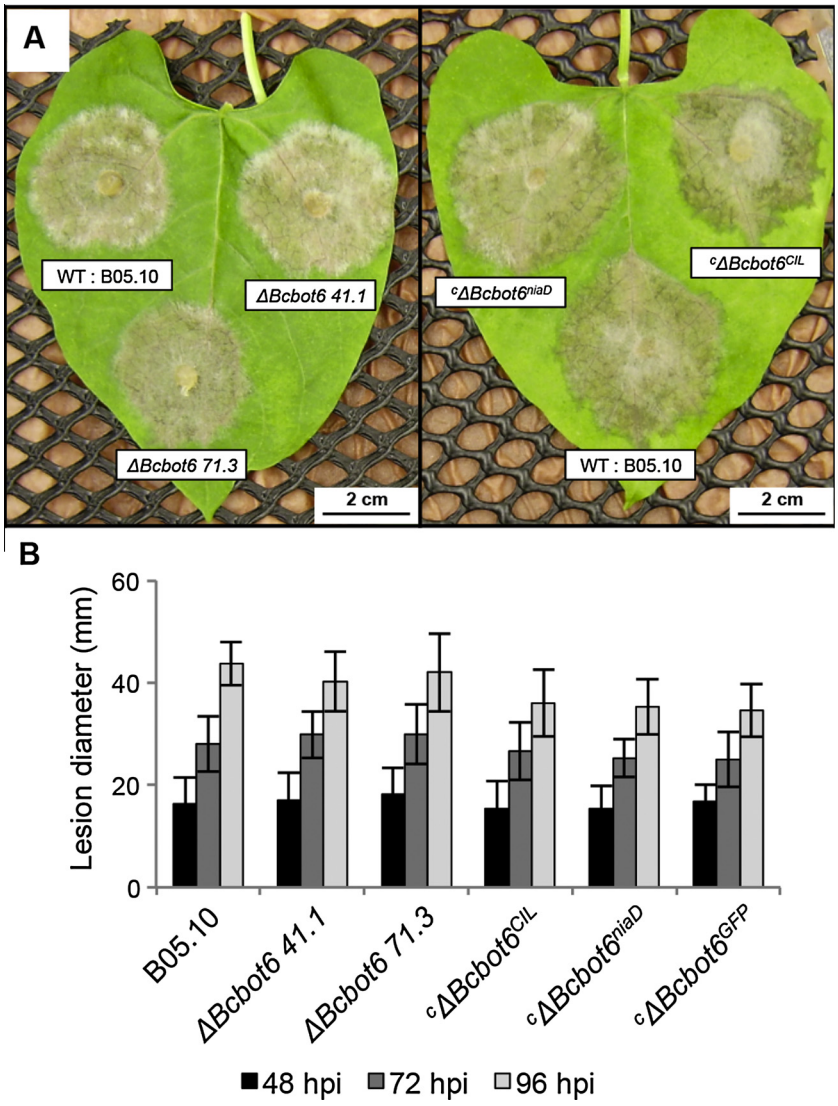


**Fig. 4.** The deletion of *Bcbot6* gene does not alter the virulence of B05.10. The virulence of the mutant *ΔBcbot6* as well as the complemented strain *$^{c}$ΔBcbot6* was evaluated on detached leaves of French bean plants (*Phaseolus vulgaris* cv. Caruso grown under glasshouse conditions) inoculated with three days-old mycelial plugs and incubated at 75% relative humidity with a photoperiod of 16 h of white light at 22 °C and 8 h of darkness at 18 °C. (A) Pictures were taken 72 hpi. (B) The virulence of the different strains was monitored from at least ten symptoms observed during two independent assays and was estimated by lesion diameters means and standard deviations. Statistical (*t*-test) analysis did not reveal significant differences between the lesions caused by the transformants and the WT strain B05.10.

the deletion of the gene dramatically impacted the expression of all *Bcbot* genes and led to the inability of the strain to produce BOT, thereby indicating that BcBot6 is a positive regulator of the BOT gene cluster. Moreover, the qRT-PCR results allowed us to determine that the BOT cluster is composed of seven genes (from *Bcbot1* to *Bcbot7*). With the present study, five *Bcbot* genes have now been characterized (Table 1). The two remaining genes whose role in BOT production has still to be confirmed are *Bcbot5* and *Bcbot7*. BcBot5 is thought to be responsible for the introduction of the acetyl group characteristic of BOT (Collado and Viaud, 2016) whereas BcBot7, which is predicted to be a dehydrogenase, might be involved in the conversion of BOT to dihydrobotrydial. As the deletion of *Bcbot6* has no impact on *Bcboa6* and *Bcpks7* expression, development and aggressivity, and does not affect the ability of the fungus to produce other metabolites, it strongly suggests that BcBot6 is a BOT pathway-specific regulator. Nevertheless, we cannot exclude that it could also regulate other genes in the genome. An interesting example is the ability of the AflR TF to regulate not only genes of the aflatoxin gene cluster in *Aspergillus parasiticus* but also additional genes outside "its" cluster (Price et al., 2006). Thus, to determine the specific regulation of the BOT gene cluster by BcBot6, a global transcriptomic assay would be necessary. A further study would also be required to identify possible DNA-binding motifs. For this purpose, we carried out a yeast one hybrid (Y1H) strategy (Fig. S7) but it failed to confirm a direct interaction between the BcBot6 and the bidirectional promoter of *Bcbot1* and *2*, probably due to technical issues such as sensitivity problems. It is also possible that, in this heterologous system, the BcBot6 TF lacks some post-translational modifications or some additional partners to bind its target DNA motif. In conclusion, even if we cannot exclude that the regulation is indirect, the most probable hypothesis is that BcBot6 is a TF acting directly on the promoter of its targeted genes.

It is well known that fungal SMs production is also governed by higher hierarchically acting signal transduction pathways. Notably, the BOT gene cluster has previously been reported to be under the control of both the calcineurin and the stress-induced MAP kinase cascade (Viaud et al., 2016). To gain insight into the whole

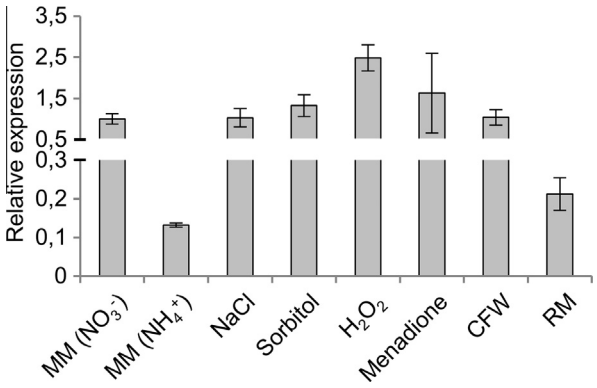


**Fig. 5.** The expression of the botrydial key enzyme-encoding gene *Bcbot2* is affected by the nitrogen source. The expression of *Bcbot2* was monitored by RT-qPCR in the WT strain B05.10 grown 96 h at 23 °C with a photoperiod of 14 h of darkness and 10 h of white light. The solid minimal medium (MM) that contains 25 mM $NaNO_3$ was used as a control condition and was supplemented with either NaCl (0.7 M), sorbitol (0.7 M), $H_2O_2$ (5 mM), menadione (300 μM) or calcofluor white (50 mg/L). Moreover, a MM in which nitrate was replaced by ammonium (12.5 mM $(NH_4)_2SO_4$) was also used, as well as the RM medium. All plates were covered with a cellophane overlay before fungus inoculation. The relative expressions were obtained with the $2^{-\Delta\Delta Ct}$ method (Livak and Schmittgen, 2001) using the constitutively expressed actin-encoding gene *BcactA* (Bcin16g02020) as a reference. The data were obtained from at least two biological replicates and from at least two technical replicates. Error bars are represented by SEM.

activation process, there is a general need to connect the specific activation of the cluster with those previously characterized pathways. In particular, the repression of the *Bcbot2* gene expression by ammonium suggests that the nitrogen source may have an important role as already described for other fungal SMs (Tudzynski, 2014). For example, the production of aflatoxin is repressed by nitrate but induced by ammonium in *A. parasiticus* and *A. flavus* (Feng and Leonard, 1998; Ehrlich et al., 2002; Tudzynski, 2014). In addition, it has been shown that the major actor of this mechanism *i.e.* the GATA TF AreA is involved in the regulation of several SM clusters in different fungal species (Tudzynski, 2014). Moreover, the direct interaction of AreA and the intergenic region of the regulatory genes AflR and AflJ was proven in *A. parasiticus* (Chang et al., 2000). The ortholog of AreA in *B. cinerea* remains to be characterized to determine its implication in the nitrogen-dependent regulation of the BOT gene cluster. One interesting clue is the presence of several AreA binding motifs (HGATAR; Ravagnani et al., 1997) into the promoter region of *Bcbot6* (data not shown). Other environmental stimuli likely influence the *Bcbot* genes expression. Nevertheless, our results did not reveal a significant impact of the osmotic or cell wall stresses on *Bcbot2* expression. Only the $H_2O_2$ treatment suggests a moderate positive effect of oxidative stress on the BOT gene cluster. This result is in agreement with the previous characterization of the stress-activated MAP kinase BcSak1: both BOT and BOA phytotoxins are produced in much lower quantities in axenic cultures of the Δ*Bcsak1* mutant compared to the WT (Heller et al., 2012). It is likely that the BcSak1 pathway regulates the expression of the *Bcbot* genes in response to oxidative stress even though there is no evidence that the known downstream TF *i.e.* BcAtf1 directly acts on the BOT gene cluster (Temme et al., 2012).

### 4.2. The BOT gene cluster is in a genomic locus with a bipartite structure

As raised above, the PacBio sequencing technology allowed a better definition of the BOT gene cluster genomic region (van Kan et al., 2016). It is now clear that the cluster is located on chromosome 12 (BCIN12) at approximately 100 kb from the telomeric end. Two A + T-rich regions (above 80% of A + T) are present upstream from the BOT gene cluster and between *Bcbot5* and *Bcbot6* genes. This particular genomic environment has already been described for the solanapyrone gene cluster in *Ascochyta rabiei* (Kim et al., 2015). In their study, the authors pointed out the presence of *Tcl/Mariner*-type TEs and further demonstrated that those sequences probably underwent the action of RIP resulting in A + T-rich regions. For the BOT gene cluster, we hypothesized that the surrounding A + T-rich regions might result from a similar mechanism. On the first hand, we undertook the annotation of the TEs on the whole *B. cinerea* gapless genome. We found that TEs represent 3.72% of the genome, what is consistent with the data published on the first versions of the genomes of B05.10 and T4 strains (Amselem et al., 2011). Moreover, the same families of retrotransposons (such as *Boty)* and DNA transposons (such as *Flipper)* were, once more, identified. Regarding the BOT gene cluster, fifteen degenerated TEs were identified and they were all but one in the A + T-rich regions devoid of genes. Furthermore, we calculated the two main RIP indices bias in *B. cinerea* (mutation from C to T in CA and CT dinucleotide; Amselem et al., 2015). Both RIP indices increase in those regions, suggesting that the TEs-containing A + T-rich regions may have undergone RIP action. RIP may have also acted on some precise parts of the G + C/A + T-equilibrated regions as RIP indices were increasing concomitantly with an increase in A + T content notably in the promoter regions of the *Bcbot4* gene. Even if most of the TEs detected in fungal genomes are inactive, they probably had a great impact on gene function and genome structure during genome evolution (Kazazian, 2004; Ayarpadikannan and Kim, 2014). As repeated sequences, they might allow genomic rearrangements by homologous recombination. Moreover, RIP is acting on targeted repeated regions but might sometimes act on flanking sequences (Ohm et al., 2012). In this case, those latter would evolve rapidly and there are accumulating evidences showing that this mechanism gives rise to new pathogenicity-related effector genes alleles. Finally, it has been shown that DIM-5 is able to generate repressive heterochromatin from RIPed A + T-rich sequences in *N. crassa* (Lewis et al., 2009). These three different reasons strongly suggest that TEs have likely played a major role in the BOT gene cluster history.

Interestingly, the SM gene cluster responsible for the second important phytotoxin of *B. cinerea*, BOA, also displays a similar bipartite structure as the BOT genomic region: TEs-containing A + T-rich regions are present both within and downstream from the *Bcboa* genes. In addition, this cluster is located in a subtelomeric region (about 4 kb from one telomere of chromosome BCIN01) (van Kan et al., 2016). Intriguingly, we were able to visualize this kind of bipartite structure for only a restricted number of SM clusters in *B. cinerea* (eight out of 40; data not shown). This raises the question whether this particular organization has an impact on chromatin structure and if it might be related to a chromatin-based regulation mechanism.

### 4.3. The role of botrydial and other botryanes remains enigmatic

Botrydial has a powerful phytotoxic activity observable on bean leaves at concentration as low as 1 ppm but in infected plants, this concentration could reach approximately 50 ppm (Deighton et al., 2001; Colmenares et al., 2002). The cellular target of BOT remains unknown but the recent work of Rossi et al. (2011) on *Arabidopsis thaliana* suggests that BOT induces the hypersensitive response through the salicylic acid and jasmonic acid signaling pathways, thereby acting as an effector of plant cell death. This biological activity fits with the available transcriptomic data: the BOT gene cluster is up-regulated during infection of different hosts including *A. thaliana* and *Vitis vinifera* (Gioti et al., 2006; Kelloniemi et al., 2015). In this study, we confirmed that the oxidative stress which

is known to occur during infection is a signal that leads to the activation of the BOT gene cluster. Additionally, we showed that ammonium strongly represses this SM gene cluster. One hypothesis to explain this repression is that this nitrogen source may act as a signal perceived by *B. cinerea* leading to a saprophytic development in which the phytotoxin production is not required.

Despite the phytotoxic activity of BOT, we demonstrated that this sesquiterpene is not necessary for the virulence of the strain B05.10. Indeed, the dramatic decrease of *Bcbot* genes expression in the *ΔBcbot6* and the subsequent absence of BOT production did not alter the development of symptoms on bean leaves. This result is in agreement with previous studies. To summarize, the deletion of either *Bcbot1*, *2*, *3*, *4 or 6* gene in the B05.10 strain and the subsequent suppression of BOT production do not affect the virulence whereas in the T4 strain, the *ΔBcbot1* and *ΔBcbot2* mutants led to smaller lesions than the WT strain (Siewers et al., 2005; Pinedo et al., 2008). The current hypothesis to explain this difference is that in the strain B05.10, the absence of BOT is supplied by the presence of BOA, whereas the T4 strain never produces this second phytotoxin. The functional redundancy of BOT and BOA toxins in B05.10 genetic background was confirmed by the inability for the *ΔBcbot2 ΔBcboa6* double mutants to fully colonize plant tissues (Dalmais et al., 2011). As for the previously characterized *ΔBcbot2* (Pinedo et al., 2008), we observed that the absence of BOT production led to a greater production of botcinins: after 12 days of axenic cultures, the *ΔBcbot6* accumulates twice as much botcinins as does the WT strain. The lack of botryanes production coupled with the enhancement of botcinins production in the *ΔBcbot6* mutant remains currently unexplained. This might contribute to the absence of virulence defect in the *ΔBcbot6* mutant, and might also account for the other results of phenotypic tests designed to test the response to different stresses.

Additional clues regarding the role of SM could arise from the study of their distribution among the fungal populations and species. All *B. cinerea* strains tested to date, *i.e.* more than fourteen, produce BOT (Reino et al., 2004; Siewers et al., 2005), suggesting that this compound has an important role in the fitness of this polyphagous species. Our molecular screening confirmed that *Bcbot2*, the BOT key enzyme-encoding gene is present in all *B. cinerea* strains tested, and further revealed that the closest species of *B. cinerea*, *i.e. B. fabae* and *B. pseudocinerea* are unable to produce BOT and other botryanes. *B. cinerea* and *B. pseudocinerea* constitute a complex of two cryptic species living in sympatry on several hosts, including grapevine and blackberry. They cannot be discriminated by morphologic criteria or by their aggressiveness on leaves. Nevertheless, a population survey over time showed that *B. cinerea* was the predominant species on mature grape berries whereas *B. pseudocinerea* was more abundant in spring, on floral debris (Walker et al., 2011). Differences in the repertoires of phytotoxic secondary metabolites might contribute to the adaptation to these different ecological niches.

Even though *Botrytis* species closely related to *B. cinerea* do not possess the key enzyme of the BOT biosynthesis pathway, botryanes compounds have been isolated from more distant species *i.e. B. squamosa* and *B. allii* which are both pathogenic towards *Allium* species (Collado et al., 2000). In our study, the detection of the *Bcbot2* gene in *B. aclada* and *B. porri* suggested that these two additional pathogens of *Allium* may also produce BOT and/or other botryanes even if that remains to be confirmed by chemical analyses. Strikingly, botryanes are also produced *in vitro* by the non-pathogenic species *Hymenoscyphus epiphyllus* that belongs to the Leotiomycetes class as *Botrytis* (Thines et al., 1997). Additionally, a SM gene cluster containing the orthologs of *Bcbot1* to *Bcbot6* was recently found in the genomes of two *Colletotrichum* species (Sordariomycetes), *C. tofieldiae* and *C. incanum* which are endophytic and pathogenic of *A. thaliana*, respectively (Hacquard et al., 2016; Hiruma et al., 2016). Remarkably, the orthologs of three genes (*Bcaba1* to *Bcaba3*) known to be involved in abscisic acid (ABA) production in *B. cinerea* are embedded in the orthologs of *Bcbot* genes in those two *Colletotrichum* species (Hacquard et al., 2016). All together, these data suggest that botryanes may be produced by phylogenetically distant fungi and that the BOT gene cluster was subjected to several genomic rearrangements. This cluster might originate from a common ancestor of Leotiomycetes and Sordariomycetes and might have been lost from the majority of species or, alternatively, the cluster may have been subjected to horizontal gene transfer between different species as demonstrated for several fungal SM gene clusters (Wisecaver and Rokas, 2015).

From a functional point of view, it now seems clear that compounds with botryane skeletons are not specifically produced by *B. cinerea* even if it remains possible that BOT itself is only produced by the gray mold agent. The ability of non- phytopathogenic fungi to produce botryanes suggests that some of these compounds may have other biological activities than phytotoxicity. Indeed, except BOT, characterized botryanes exhibit only a weak phytotoxic activity (Collado et al., 1996, 1999; Durán-Patrón et al., 1999; Colmenares et al., 2002). Nevertheless, several botryanes from *Botrytis* spp and *H. epiphyllus* exhibit antibacterial and antifungal activities (Thines et al., 1997; Durán-Patrón et al., 1999). BOT has been reported to have antimicrobial activity on *Bacillus subtilis* and *Pythium debaryanum* (Fehlhaber et al., 1974; Durán-Patrón et al., 1999). In addition, BOT seems to be toxic for *B. cinerea* itself as the application of exogenous metabolite (50–250 ppm) inhibits the growth of the fungus (Durán-Patrón et al., 2004). Finally, a recent study by Malmierca et al. (2016) proposes that BOT may be involved in the communication with other microorganisms. Indeed, confrontation assays with *Trichoderma arundinaceum* suggest that BOT has a role in limiting the production of the sesquiterpene harzianum A. It thus appears that botryanes including BOT are metabolites with activities against a broad range of organisms, suggesting that they may have a wider ecological role than phytotoxicity.

To conclude, we provide here a significant expansion of the BOT gene cluster. The functional characterization of BcBot6 confirmed our hypothesis regarding its regulation role of the *Bcbot* genes in a likely specific manner. Nonetheless, much remains to be discovered regarding this cluster, especially the regulation by broad domain TFs in response to environmental stimuli and by putative chromatin-based mechanisms remain to be explored. Deciphering the complex regulation of this metabolite synthesis would help to define its role in the interactions with plants and other organisms.

## Acknowledgments

The authors would like to thank Samy Hamadache for the pathotests and evaluation of the growth under different stress conditions. We also warmly thank Julia Schumacher (University of Muenster, Germany) for sharing the pNDN-OGG vector and Ralph Dean (North Carolina State University) for critical reading of the manuscript. This research did not receive any specific grant from funding agencies in the public, commercial, or not-for-profit sectors. The authors declare no conflict of interest.

## Appendix A. Supplementary material

Supplementary data associated with this article can be found, in the online version, at http://dx.doi.org/10.1016/j.fgb.2016.10.003.

## References


Amselem, J., Cuomo, C.A., van Kan, J.A.L., Viaud, M., Benito, E.P., Couloux, A., et al., 2011. Genomic analysis of the necrotrophic fungal pathogens *Sclerotinia sclerotiorum* and *Botrytis cinerea*. PLoS Genet 7, e1002230.

Amselem, J., Lebrun, M.-H., Quesneville, H., 2015. Whole genome comparative analysis of transposable elements provides new insight into mechanisms of their inactivation in fungal genomes. BMC Genomics 16, 141.

Ayarpadikannan, S., Kim, H.-S., 2014. The impact of transposable elements in genome evolution and genetic instability and their implications in various diseases. Genomics Inform. 12, 98.

Bao, Z., Eddy, S.R., 2002. Automated *de novo* identification of repeat sequence families in sequenced genomes. Genome Res. 12, 1269–1276.

Bayram, O., Krappmann, S., Ni, M., Bok, J.W., Helmstaedt, K., Valerius, O., et al., 2008. VelB/VeA/LaeA complex coordinates light signal with fungal development and secondary metabolism. Science 320, 1504–1506.

Brakhage, A.A., 2012. Regulation of fungal secondary metabolism. Nat. Rev. Microbiol. 11, 21–32.

Calvo, A.M., Wilson, R.A., Bok, J.W., Keller, N.P., 2002. Relationship between secondary metabolism and fungal development. Microbiol. Mol. Biol. Rev. 66, 447–459.

Catlett, N.L., Lee, B.-N., Yoder, O.C., Turgeon, B.G., 2003. Split-marker recombination for efficient targeted deletion of fungal genes. Fungal Genet News 50, 9–11.

Chang, P.-K., Yu, J., Bhatnagar, D., Cleveland, T.E., 2000. Characterization of the *Aspergillus parasiticus* major nitrogen regulatory gene, areA. Biochim. Biophys. Acta BBA – Gene Struct. Expr. 1491, 263–266.

Collado, I.G., Aleu, J., Hernández-Galán, R., Durán-Patrón, R., 2000. Botrytis species an intriguing source of metabolites with a wide range of biological activities. Structure, chemistry and bioactivity of metabolites isolated from Botrytis species. Curr. Org. Chem. 4, 1261–1286.

Collado, I.G., Durán-Patrón, R., Hernández-Galán, R., 1999. Some evidence on the role of exudated toxins in the pathogenesis of *Botrytis cinerea*. Rec. Adv. Allelopathy 1, 479–484.

Collado, I.G., Hernández-Galán, R., Prieto, V., Hanson, J.R., Rebordinos, L.G., 1996. Biologically active sesquiterpenoid metabolites from the fungus *Botrytis cinerea*. Phytochemistry 41, 513–517.

Collado, I.G., Sánchez, A.J.M., Hanson, J.R., 2007. Fungal terpene metabolites: biosynthetic relationships and the control of the phytopathogenic fungus Botrytis cinerea. Nat. Prod. Rep. 24, 674–686.

Collado, I.G., Viaud, M., 2016. Secondary metabolism in botrytis cinerea: combining genomic and metabolomic approaches. In: Fillinger, S., Elad, Y. (Eds.), Botrytis – The Fungus, the Pathogen and Its Management in Agricultural Systems. Springer International Publishing, pp. 291–313.

Colmenares, A.J., Aleu, J., Durán-Patrón, R., Collado, I.G., Hernández-Galán, R., 2002. The putative role of botrydial and related metabolites in the infection mechanism of *Botrytis cinerea*. J. Chem. Ecol. 28, 997–1005.

Colot, H.V., Park, G., Turner, G.E., Ringelberg, C., Crew, C.M., Litvinkova, L., et al., 2006. A high-throughput gene knockout procedure for Neurospora reveals functions for multiple transcription factors. Proc. Natl. Acad. Sci. USA 103, 10352–10357.

Cutler, H.G., Jacyno, M.J., Harwood, S.J., Dulik, D., Goodrich, D.P., Roberts, G.R., 1993. Botcinolide: a biologically active natural product from *Botrytis cinerea*. Biosci. Biotechnol. Biochem. 57, 1980–1982.

Cutler, H.G., Parker, S.R., Ross, S.A., Crumley, F.G., Schreiner, P.R., 1996. Homobotcinolide: a biologically active natural homolog of botcinolide from *Botrytis cinerea*. Biosci. Biotechnol. Biochem. 60, 656–658.

Dalmais, B., Schumacher, J., Moraga, J., Le Pêcheur, P., Tudzynski, B., Collado, I.G., Viaud, M., 2011. The *Botrytis cinerea* phytotoxin botcinic acid requires two polyketide synthases for production and has a redundant role in virulence with botrydial: Botcinic acid biosynthesis gene clusters. Mol. Plant Pathol. 12, 564–579.

Dean, R., Van Kan, J.A.L., Pretorius, Z.A., Hammond-Kosack, K.E., Di Pietro, A., Spanu, P.D., et al., 2012. The Top 10 fungal pathogens in molecular plant pathology: Top 10 fungal pathogens. Mol. Plant Pathol. 13, 414–430.

Deighton, N., Muckenschnabel, I., Colmenares, A.J., Collado, I.G., Williamson, B., 2001. Botrydial is produced in plant tissues infected by *Botrytis cinerea*. Phytochemistry 57, 689–692.

Durán-Patrón, R., Cantoral, J.M., Hernández-Galán, R., Hanson, J.R., Collado, I.G., 2004. The biodegradation of the phytotoxic metabolite botrydial by its parent organism, *Botrytis cinerea*. J. Chem. Res. 2004, 441–443.

Durán-Patrón, R., Hernández-Galán, R., Rebordinos, L.G., Cantoral, J.M., Collado, I.G., 1999. Structure-activity relationships of new phytotoxic metabolites with the botryane skeleton from *Botrytis cinerea*. Tetrahedron 55, 2389–2400.

Edgar, R.C., Myers, E.W., 2005. PILER: identification and classification of genomic repeats. Bioinformatics 21, i152–i158.

Ehrlich, K.C., Montalbano, B.G., Cary, J.W., Cotty, P.J., 2002. Promoter elements in the aflatoxin pathway polyketide synthase gene. Biochim. Biophys. Acta BBA – Gene Struct. Expr. 1576, 171–175.

Eisenman, H.C., Casadevall, A., 2012. Synthesis and assembly of fungal melanin. Appl. Microbiol. Biotechnol. 93, 931–940.

Elad, Y., Pertot, I., Cotes Prado, A.M., Stewart, A., 2016. Plant hosts of botrytis spp. In: Fillinger, S., Elad, Y. (Eds.), Botrytis – the Fungus, the Pathogen and Its Management in Agricultural Systems. Springer International Publishing, Cham, pp. 413–486.

Fairhead, C., Llorente, B., Denis, F., Soler, M., Dujon, B., 1996. New vectors for combinatorial deletions in yeast chromosomes and for gap-repair cloning using "split-marker" recombination. Yeast 12, 1439–1457.

Fehlhaber, H.-W., Geipel, R., Mercker, H.-J., Tschesche, R., Welmar, K., Schönbeck, F., 1974. Botrydial, ein Sesquiterpen-Antibiotikum aus der Nährlösung des Pilzes *Botrytis cinerea*. Chem. Ber. 107, 1720–1730.

Feng, G.H., Leonard, T.J., 1998. Culture conditions control expression of the genes for aflatoxin and sterigmatocystin biosynthesis in *Aspergillus parasiticus* and *A. nidulans*. Appl. Environ. Microbiol. 64, 2275–2277.

Flutre, T., Duprat, E., Feuillet, C., Quesneville, H., 2011. Considering transposable element diversification in *de novo* annotation approaches. PLoS ONE 6, e16526.

Gao, F., Zhang, C.-T., 2006. GC-Profile: a web-based tool for visualizing and analyzing the variation of GC content in genomic sequences. Nucleic Acids Res. 34, W686–W691.

Gioti, A., Simon, A., Le Pêcheur, P., Giraud, C., Pradier, J.M., Viaud, M., Levis, C., 2006. Expression profiling of *Botrytis cinerea* genes identifies three patterns of up-regulation in planta and an FKBP12 protein affecting pathogenicity. J. Mol. Biol. 358, 372–386.

Hacquard, S., Kracher, B., Hiruma, K., Münch, P.C., Garrido-Oter, R., Thon, M.R., et al., 2016. Survival trade-offs in plant roots during colonization by closely related beneficial and pathogenic fungi. Nat. Commun. 7, 11362.

Hane, J.K., Oliver, R.P., 2008. RIPCAL: a tool for alignment-based analysis of repeat-induced point mutations in fungal genomic sequences. BMC Bioinformatics 9, 478.

Hane, J.K., Williams, A.H., Taranto, A.P., Solomon, P.S., Oliver, R.P., 2015. Repeat-induced point mutation: a fungal-specific, endogenous mutagenesis process. In: Berg, M.A. van den, Maruthachalam, K. (Eds.), Genetic Transformation Systems in Fungi, Fungal Biology, vol. 2. Springer International Publishing, pp. 55–68.

Heller, J., Ruhnke, N., Espino, J.J., Massaroli, M., Collado, I.G., Tudzynski, P., 2012. The mitogen-activated protein kinase BcSak1 of *Botrytis cinerea* is required for pathogenic development and has broad regulatory functions beyond stress response. Mol. Plant. Microbe Interact. 25, 802–816.

Hiruma, K., Gerlach, N., Sacristán, S., Nakano, R.T., Hacquard, S., Kracher, B., et al., 2016. Root endophyte colletotrichum tofieldiae confers plant fitness benefits that are phosphate status dependent. Cell.

Hoede, C., Arnoux, S., Moisset, M., Chaumier, T., Inizan, O., Jamilloux, V., Quesneville, H., 2014. PASTEC: an automatic transposable element classification tool. PLoS ONE 9, e91929.

Hoffmeister, D., Keller, N.P., 2007. Natural products of filamentous fungi: enzymes, genes, and their regulation. Nat. Prod. Rep. 24, 393.

Jurka, J., Kapitonov, V.V., Pavlicek, A., Klonowski, P., Kohany, O., Walichiewicz, J., 2005. Repbase update, a database of eukaryotic repetitive elements. Cytogenet. Genome Res. 110, 462–467.

van Kan, J.A.L., Stassen, J.H.M., Mosbach, A., Van Der Lee, T.A.J., Faino, L., Farmer, A. D., et al., 2016. A gapless genome sequence of the fungus *Botrytis cinerea*. Mol. Plant Pathol. http://dx.doi.org/10.1111/mpp.12384.

Kangatharalingam, N., Ferguson, M.W., 1984. A simple and rapid technique for fluorescence staining of fungal nuclei. Curr. Microbiol. 10, 99–103.

Kazazian, H.H., 2004. Mobile elements: drivers of genome evolution. Science 303, 1626–1632.

Keller, N.P., Hohn, T.M., 1997. Metabolic pathway gene clusters in filamentous fungi. Fungal Genet. Biol. 21, 17–29.

Kelloniemi, J., Trouvelot, S., Héloir, M.-C., Simon, A., Dalmais, B., Frettinger, P., et al., 2015. Analysis of the molecular dialogue between gray mold (*Botrytis cinerea*) and grapevine (*Vitis vinifera*) reveals a clear shift in defense mechanisms during berry ripening. Mol. Plant. Microbe Interact. 28, 1167–1180.

Kim, H., Woloshuk, C.P., 2008. Role of AREA, a regulator of nitrogen metabolism, during colonization of maize kernels and fumonisin biosynthesis in *Fusarium verticillioides*. Fungal Genet. Biol. 45, 947–953.

Kim, W., Park, J.-J., Gang, D.R., Peever, T.L., Chen, W., 2015. A novel type pathway-specific regulator and dynamic genome environments of a solanapyrone biosynthesis gene cluster in the Fungus *Ascochyta rabiei*. Eukaryot. Cell 14, 1102–1113.

Knox, B.P., Keller, N.P., 2015. Key players in the regulation of fungal secondary metabolism. In: Zeilinger, S., Martín, J.-F., García-Estrada, C. (Eds.), Biosynthesis and Molecular Genetics of Fungal Secondary Metabolites, vol. 2. Springer, New York, New York, NY, pp. 13–28.

Leroch, M., Mernke, D., Koppenhoefer, D., Schneider, P., Mosbach, A., Doehlemann, G., Hahn, M., 2011. Living colors in the gray mold pathogen *Botrytis cinerea*: codon-optimized genes encoding green fluorescent protein and mcherry, which exhibit bright fluorescence. Appl. Environ. Microbiol. 77, 2887–2897.

Levis, C., Fortini, D., Brygoo, Y., 1997. Transformation of *Botrytis cinerea* with the nitrate reductase gene (niaD) shows a high frequency of homologous recombination. Curr. Genet. 32, 157–162.

Lewis, Z.A., Honda, S., Khlafallah, T.K., Jeffress, J.K., Freitag, M., Mohn, F., et al., 2009. Relics of repeat-induced point mutation direct heterochromatin formation in *Neurospora crassa*. Genome Res. 19, 427–437.

Livak, K.J., Schmittgen, T.D., 2001. Analysis of relative gene expression data using real-time quantitative PCR and the $2^{-\Delta\Delta C_T}$ Method. Methods 25, 402–408.

Malmierca, M.G., Izquierdo-Bueno, I., McCormick, S.P., Cardoza, R.E., Alexander, N.J., Moraga, J., et al., 2016. Botrydial and botcinins produced by *Botrytis cinerea* regulate expression of *Trichoderma arundinaceum* genes involved in trichothecene biosynthesis: fungal metabolites cross-regulation. Mol. Plant Pathol. http://dx.doi.org/10.1111/1462-2920.13410.

Manzoni, M., Rollini, M., 2002. Biosynthesis and biotechnological production of statins by filamentous fungi and application of these cholesterol-lowering drugs. Appl. Microbiol. Biotechnol. 58, 555–564.
Medema, M.H., Kottmann, R., Yilmaz, P., Cummings, M., Biggins, J.B., Blin, K., et al., 2015. Minimum Information about a Biosynthetic Gene cluster. Nat. Chem. Biol. 11, 625–631.
Michielse, C.B., Becker, M., Heller, J., Moraga, J., Collado, I.G., Tudzynski, P., 2011. The *Botrytis cinerea* Reg1 Protein, a putative transcriptional regulator, is required for pathogenicity, conidiogenesis, and the production of secondary metabolites. Mol. Plant. Microbe Interact. 24, 1074–1085.
Moraga, J., Dalmais, B., Izquierdo-Bueno, I., Aleu, J., Hanson, J.R., Hernández-Galán, R., et al., 2016. Genetic and molecular basis of botrydial biosynthesis. Connecting cytochrome P450-encoding genes to biosynthetic intermediates. ACS Chem. Biol.
Mutterer, J., Zinck, E., 2013. Quick-and-clean article figures with FigureJ. J. Microsc. 252, 89–91.
Ohm, R.A., Feau, N., Henrissat, B., Schoch, C.L., Horwitz, B.A., Barry, K.W., et al., 2012. Diverse lifestyles and strategies of plant pathogenesis encoded in the genomes of eighteen dothideomycetes fungi. PLOS Pathog 8, e1003037.
Palmer, J.M., Keller, N.P., 2010. Secondary metabolism in fungi: does chromosomal location matter? Curr. Opin. Microbiol. 13, 431–436.
Pinedo, C., Wang, C.-M., Pradier, J.-M., Dalmais, B., Choquer, M., Le Pêcheur, P., et al., 2008. Sesquiterpene synthase from the botrydial biosynthetic gene cluster of the phytopathogen *Botrytis cinerea*. ACS Chem. Biol. 3, 791–801.
Price, M.S., Yu, J., Nierman, W.C., Kim, H.S., Pritchard, B., Jacobus, C.A., et al., 2006. The aflatoxin pathway regulator AflR induces gene transcription inside and outside of the aflatoxin biosynthetic cluster. FEMS Microbiol. Lett. 255, 275–279.
Quesneville, H., Bergman, C.M., Andrieu, O., Autard, D., Nouaud, D., Ashburner, M., Anxolabehere, D., 2005. Combined evidence annotation of transposable elements in genome sequences. PLOS Comput. Biol. 1, e22.
Quidde, T., Osbourn, A., Tudzynski, P., 1998. Detoxification of α-tomatine by *Botrytis cinerea*. Physiol. Mol. Plant Pathol. 52, 151–165.
Ravagnani, A., Gorfinkiel, L., Langdon, T., Diallinas, G., Adjadj, E., Demais, S., et al., 1997. Subtle hydrophobic interactions between the seventh residue of the zinc finger loop and the first base of an HGATAR sequence determine promoter-specific recognition by the *Aspergillus nidulans* GATA factor AreA. EMBO J. 16, 3974–3986.
Rebordinos, L., Cantoral, J.M., Prieto, M.V., Hanson, J.R., Collado, I.G., 1996. The phytotoxic activity of some metabolites of *Botrytis cinerea*. Phytochemistry 42, 383–387.
Reino, J.L., Durán-Patrón, R., Segura, I., Hernández-Galán, R., Riese, H.H., Collado, I.G., 2003. Chemical transformations on botryane skeleton. Effect on the cytotoxic activity. J. Nat. Prod. 66, 344–349.
Reino, J.L., Hernández-Galán, R., Durán-Patrón, R., Collado, I.G., 2004. Virulence-toxin production relationship in isolates of the plant pathogenic fungus *Botrytis cinerea*. J. Phytopathol. 152, 563–566.
Reyes-Dominguez, Y., Bok, J.W., Berger, H., Shwab, E.K., Basheer, A., Gallmetzer, A., et al., 2010. Heterochromatic marks are associated with the repression of secondary metabolism clusters in *Aspergillus nidulans*: heterochromatin regulation of secondary metabolism. Mol. Microbiol. 76, 1376–1386.
Rohlfs, M., Churchill, A.C.L., 2011. Fungal secondary metabolites as modulators of interactions with insects and other arthropods. Fungal Genet. Biol. 48, 23–34.
Rossi, F.R., Gárriz, A., Marina, M., Romero, F.M., Gonzalez, M.E., Collado, I.G., Pieckenstain, F.L., 2011. The sesquiterpene botrydial produced by *Botrytis cinerea* induces the hypersensitive response on plant tissues and its action is modulated by salicylic acid and jasmonic acid signaling. Mol. Plant. Microbe Interact. 24, 888–896.
Schumacher, J., 2008a. Calcineurin-responsive zinc finger transcription factor CRZ1 of *Botrytis cinerea* Is required for growth, development, and full virulence on bean plants. Eukaryot. Cell 7, 584–601.
Schumacher, J., 2016. DHN melanin biosynthesis in the plant pathogenic fungus *Botrytis cinerea* is based on two developmentally regulated key enzyme (PKS)-encoding genes: DHN melanogenesis in *Botrytis cinerea*. Mol. Microbiol. 99, 729–748.
Schumacher, J., 2008b. The Gα subunit BCG1, the phospholipase C (BcPLC1) and the calcineurin phosphatase co-ordinately regulate gene expression in the grey mould fungus *Botrytis cinerea*. Mol. Microbiol. 67, 1027–1050.
Schumacher, J., 2012. Tools for *Botrytis cinerea*: new expression vectors make the gray mold fungus more accessible to cell biology approaches. Fungal Genet. Biol. 49, 483–497.
Schumacher, J., Pradier, J.-M., Simon, A., Traeger, S., Moraga, J., Collado, I.G., et al., 2012. Natural variation in the VELVET Gene bcvel1 affects virulence and light-dependent differentiation in *Botrytis cinerea*. PLoS ONE 7, e47840.
Schumacher, J., Simon, A., Cohrs, K.C., Traeger, S., Porquier, A., Dalmais, B., et al., 2015. The VELVET complex in the gray mold fungus *Botrytis cinerea*: impact of BcLAE1 on differentiation, secondary metabolism and virulence. Mol. Plant. Microbe Interact.
Siewers, V., Viaud, M., Jimenez-Teja, D., Collado, I.G., Gronover, C.S., Pradier, J.-M., et al., 2005. Functional analysis of the cytochrome P450 monooxygenase gene bcbot1 of *Botrytis cinerea* indicates that botrydial is a strain-specific virulence factor. Mol. Plant. Microbe Interact. 18, 602–612.
Simon, A., Dalmais, B., Morgant, G., Viaud, M., 2013. Screening of a *Botrytis cinerea* one-hybrid library reveals a $Cys_2His_2$ transcription factor involved in the regulation of secondary metabolism gene clusters. Fungal Genet. Biol. 52, 9–19.
Smith, D.J., Burnham, M.K., Bull, J.H., Hodgson, J.E., Ward, J.M., Browne, P., et al., 1990. Beta-lactam antibiotic biosynthetic genes have been conserved in clusters in prokaryotes and eukaryotes. EMBO J. 9, 741–747.
Staats, M., van Kan, J.A.L., 2012. Genome update of botrytis cinerea strains B05.10 and T4. Eukaryot. Cell 11, 1413–1414.
Tamaru, H., Selker, E.U., 2001. A histone H3 methyltransferase controls DNA methylation in Neurospora crassa. Nature 414, 277–283.
Temme, N., Oeser, B., Massaroli, M., Heller, J., Simon, A., GonzáLez Collado, I., et al., 2012. BcAtf1, a global regulator, controls various differentiation processes and phytotoxin production in Botrytis cinerea: BcAtf1-a global regulator in *Botrytis cinerea*. Mol. Plant Pathol. 13, 704–718.
Thines, E., Anke, H., Steglich, W., Sterner, O., 1997. New botrydial sesquiterpenoids from *Hymenoscyphus epiphyllus*. Z. Für Naturforschung C 52, 413–420.
Tudzynski, B., 2014. Nitrogen regulation of fungal secondary metabolism in fungi. Front. Microbiol. 5, 656.
Tudzynski, B., Homann, V., Feng, B., Marzluf, G.A., 1999. Isolation, characterization and disruption of the areA nitrogen regulatory gene of *Gibberella fujikuroi*. Mol. Gen. Genet. MGG 261, 106–114.
Viaud, M., Brunet-Simon, A., Brygoo, Y., Pradier, J.-M., Levis, C., 2003. Cyclophilin A and calcineurin functions investigated by gene inactivation, cyclosporin A inhibition and cDNA arrays approaches in the phytopathogenic fungus *Botrytis cinerea*: Botrytis calcineurin and cyclophilin-dependent genes. Mol. Microbiol. 50, 1451–1465.
Viaud, M., Schumacher, J., Porquier, A., Simon, A., 2016. Regulation of secondary metabolism in the gray mold fungus *Botrytis cinerea*. Host-Pathog. Interact. Microb. Metab. Pathog. Antiinfectives, 201–216.
Walker, A.-S., Gautier, A., Confais, J., Martinho, D., Viaud, M., Le Pêcheur, P., et al., 2011. *Botrytis pseudocinerea*, a new cryptic species causing gray mold in French vineyards in sympatry with *Botrytis cinerea*. Phytopathology 101, 1433–1445.
Wicker, T., Sabot, F., Hua-Van, A., Bennetzen, J.L., Capy, P., Chalhoub, B., et al., 2007. A unified classification system for eukaryotic transposable elements. Nat. Rev. Genet. 8, 973–982.
Wiemann, P., Willmann, A., Straeten, M., Kleigrewe, K., Beyer, M., Humpf, H.-U., Tudzynski, B., 2009. Biosynthesis of the red pigment bikaverin in Fusarium fujikuroi: genes, their function and regulation. Mol. Microbiol. 72, 931–946.
Wisecaver, J.H., Rokas, A., 2015. Fungal metabolic gene clusters-caravans traveling across genomes and environments. Front. Microbiol. 6, 161.
Yang, Q., Chen, Y., Ma, Z., 2013. Involvement of BcVeA and BcVelB in regulating conidiation, pigmentation and virulence in *Botrytis cinerea*. Fungal Genet. Biol. 50, 63–71.
Yin, W., Keller, N.P., 2011. Transcriptional regulatory elements in fungal secondary metabolism. J. Microbiol. 49, 329–339.
Yu, J.-H., Keller, N., 2005. Regulation of secondary metabolism in filamentous fungi. Annu. Rev. Phytopathol. 43, 437–458.